Surface response modeling of homogeneous photo Fenton Fe(III) and Fe(II) complex for sunlight degradation and mineralization of food dye

Mohammed Kebir, Imen-Kahina Benramdhan, Noureddine Nasrallah, Hichem Tahraoui, Nadia Baït, Houssine Benaissa, Rachid Ameraoui, Jie Zhang, Aymen Amin Assadi, Lotfi Mouni, et al.

Catalysis Communications 183 (2023) 106780

Contents lists available at ScienceDirect

Catalysis Communications

journal homepage: www.elsevier.com/locate/catcom

Surface response modeling of homogeneous photo Fenton Fe(III) and Fe(II) complex for sunlight degradation and mineralization of food dye

Mohammed Kebir [a], Imen-Kahina Benramdhan [b], Noureddine Nasrallah [b], Hichem Tahraoui [c,d], Nadia Bait [a], Houssine Benaissa [e], Rachid Ameraoui [f], Jie Zhang [g], Aymen Amin Assadi [h,i], Lotfi Mouni [j], Abdeltif Amrane [h,*]

[a] Research Unit in Physical and Chemical Analysis in Fluid and Solid Media (UR-APCMFS/CRAPC), BP 384 Bou-Ismail, 42000 Tipaza, Algeria
[b] Laboratory of Reaction Engineering, Faculty of Mechanical Engineering and Process Engineering USTHB, BP 32, El-Allia, Bab-Ezzouar, Algiers 16111, Algeria
[c] Laboratoire de Génie des Procédés Chimiques, Department of Process Engineering, University of Ferhat Abbas, Setif,Algeria
[d] Laboratoire de Biomatériaux et Phénomènes de Transports (LBMPT), Université Yahia Fares de Médéa Pôle Urbain, 26000 Médéa, Algeria
[e] LEC, Ecole Militaire Polytechnique BP17, BEB, 16111, Algiers, Algeria
[f] Centre de Recherche Scientifique et Technique en Analyses Physico-Chimiques CRAPC, BP 384, Bou-Ismail, 42004 Tipaza, Algeria
[g] School of Chemical Engineering and Advanced Materials, Newcastle University, Newcastle upon Tyne NE1 7RU, UK
[h] Univ Rennes, Ecole Nationale Supérieure de Chimie de Rennes, CNRS, ISCR, UMR 6226, F-35000 Rennes, France.
[i] Department of Chemistry, Al Imam Mohammad Ibn Saud Islamic University (IMISIU), P.O. Box 5701, Riyadh 11432, Saudi Arabia
[j] Laboratory of Management and Valorization of Natural Resources and Quality Assurance, SNVST Faculty, University of Bouira, 10000, Algeria

ARTICLE INFO

Keywords:
Complex
Degradation
Food dye
Mineralization
Box-Benhken design
Response surface

ABSTRACT

This study explores efficient Sicomet Green (SG) dye degradation using Fe(III)/Lig and Fe(II)/Lig complexes in modified photo-Fenton processes under UV, LED, and sunlight. Sunlight irradiation showed rapid kinetics with over 70% degradation efficiency. Multi-objective grey wolf optimization achieved 98% degradation and 96% mineralization yield using Fe(III)/Lig without pH adjustment. Inorganic ions inhibited the modified photo-Fenton process. A user-friendly app aided predictions and optimal parameters selection, emphasizing natural light sources and pH-neutral medium for dye removal through photo-Fenton.

1. Introduction

The food industry sector consumes a significant amount of water, resulting in a considerable level of pollution in the aquatic environment due to its discharged wastewater, which is heavily contaminated with colors [1]. Moreover, these discharges pose a major health hazard as most dyes are harmful to humans and environment. The treatment of such wastewater presents a significant challenge, particularly for developing countries that lack the necessary tools to incorporate sustainable development concepts effectively [2]. Dyes, with their complex chemical structures and the presence of aromatic rings with inorganic ions, are resistant to biodegradation under aerobic conditions [3]. Consequently, their aqueous effluents require special treatment due to their unique impact on the natural environment, including toxicity from the parent product and potential by-products [4]. These harmful contaminants need to be removed, and numerous biological, chemical and physical processes are employed for this purpose. However, traditional treatments such as adsorption on activated carbon or natural biosorbents, membrane processes, coagulation-flocculation, and chemical oxidations have disadvantages. For example, they transfer and concentrate the pollutants in one aqueous phase, leading to the formation of concentrated sludge [5]. Consequently, this creates a secondary waste problem. Among all the approaches that can be used, the photo-Fenton as a part of the advanced oxidation processes (AOPs) appears to be the process of choosing among all the possible treatment approaches for decontaminating aqueous organic effluents since they allow for total pollutant degradation with producing water and carbon dioxide while also lowering the effluent's overall toxicity [6,7].

Among the other advantages that encourage the choice of a water treatment process is: effectiveness and simplicity of operation with the possibility of using a wide range of light wavelengths (UV–Vis regions), in order to achieve this objective, natural sunlight is a prejudicial choice

* Corresponding author.
E-mail addresses: tahraoui.hichem@univ-Medea.dz (H. Tahraoui), jie.zhang@newcastle.ac.uk (J. Zhang), aymen.assadi@ensc-rennes.fr (A.A. Assadi), abdeltif.amrane@univ-rennes1.fr (A. Amrane).

https://doi.org/10.1016/j.catcom.2023.106780
Received 28 July 2023; Received in revised form 3 October 2023; Accepted 12 October 2023
Available online 14 October 2023

and represents a cheap source of energy [8].

Comparing the photo Fenton system with other water treatment processes, it has been shown that the use of photo Fenton has the advantage of not forming sludge, being very safe and easy to implement. In addition, it has the advantage of fast reaction.

The photo-Fenton reactions are non-selective reactive oxidizing species-based technologies that enable the oxidation of a wide variety of organic contaminants with pH ranging from 2 to 4. However, a drawback of the photo-Fenton process is the precipitation of ferric oxyhydroxide [9]. The hydroxyl radical is the most often utilized oxidant due to its high reactivity (EÂ° = 2.73 V). In both the homogeneous and heterogeneous phases, POAs exhibit a diversity of oxidation types [10].

Additionally, in the photo-Fenton process, the regeneration of Fe^{2+} ions is best promoted in the presence of certain organic acids chelates such as carboxylates, hydroxy carboxylates of amino polycarboxylates and natural organic acids. The main role of these chelates is integrated into the coordination with Fe^{3+} ions, thus inducing a photochemical reduction of Fe^{3+} to Fe^{2+} through ligand-to-metal charge transfer to generate Fe^{2+} ions [11].

These characteristics have stimulated the use of ferrioxalate in the photo-Fenton reaction with important advantages of reducing operating costs and making the photo-Fenton process very attractive for various water treatment applications. This is because the ferric-oxalate complex absorbs light energy strongly between 250 and 550 nm and limits the consumption of chemical products, providing a high quantum yield and ensuring the regeneration of ferrous iron and additional production of HO radicals [12].

On the other hand, ferrioxalate complexes allow the formation of stable complexes between ferric ions and organic species in the contaminated solution. In addition, iron precipitation is inhibited even at near-neutral pH in the presence of the ferrioxalate complex. This last point is of great interest when treating industrial effluents loaded with coloring pollutants, where the pH is generally close to neutral or alkaline [13,14].

In this work, we were interested in the removal of SG detergent dye, which poses a serious problem of water contamination due to the activity of local industry, and in our knowledge, no research has been found for the SG dye degradation by photo-Fenton process before.

However, in the study of the oxidation of the SG dye with the modified photo-Fenton homogeneous system, the reaction is done between the complex Fe(III) and a ligand under a sunlight source of irradiation as follows [9]:

$$Fe^{3+}\ (C_2O_4)_n^{(3-2n)} + hv \rightarrow Fe^{2+} + (n-1)\ C_2O_4^{2-} + C_2O_4^{2-} \quad (1)$$

While the second process of the modified photo Fenton oxidation reaction is based on the complex consisting of Fe(II), the organic ligand and the oxidant H_2O_2, the mixture is irradiated with a sunlight source, according to the following reaction:

$$Fe^{2+}C_2O_4 + H_2O_2 + hv \rightarrow Fe^{3+I}(C_2O_4)^+ + OH^{\bullet} + OH \quad (2)$$

In this way, the strategy focused in this study shows that SG organic dye widely used in the food industry, iron ligands and sunlight can potentially be used in the modified photo-Fenton treatment process to prevent iron precipitation at a neutral pH range.

A study of the parameters influencing the photo Fenton process was undertaken as well as the influence of the addition of inorganic ions and scavengers in order to approach the real effluent and to obtain a complete SG degradation and mineralization.

Moreover, a Box-Behnken statistical experiment design based on response surface analysis was applied for this context, by considering the operating parameters as the independent variables and the rate of photodegradation and mineralization as dependent variables [15]. The kinetics of photodegradation and mineralization are also investigated.

We were interested in textile dyes because they pose a real problem of water contamination due to the activity of local industry, and their degradation has received scant attention in the literature. Among all the approaches that can be used in advanced oxidation processes (AOPs), photo-Fenton appears to be the process of choice among all the possible treatment approaches for contaminated aqueous effluents since they allow for total pollutant degradation while also lowering the effluent's overall toxicity. The creation of active and non-specific species such as hydroxyl radicals is at the heart of AOPs. Photocatalysis looks to be one of the most cost-effective methods for achieving organic compound mineralization.

Additionally, this study aims to investigate the utilization of statistical analysis tools and response surface methodology for the optimization of the SG degradation process. The developed model is used to identify the optimal parameters that enhance the degradation process efficiency and yield valuable insights, despite the complexities associated with the modified photo-Fenton degradation system. The obtained optimal parameters are validated through experiments.

The paper is organized as follows. Section 2 introduces the materials and methods. Detailed results are given and discussed in Section 3. Some concluding remarks are drawn in Section 4.

2. Materials and methods

2.1. Chemicals

The chemicals reagents used in this study are Sodium bicarbonate $NaHCO_3$ (>99%, Sigma Aldrich), Sodium chloride NaCl (>99.5%, Fluka), Oxalic acid $C_2H_2O_4$ (≥99%, Merk), Isopropanol C_3H_8O (>98%, Merck), Hydrogen peroxide H_2O_2 (30% *w/v*, Sigma-Aldric), 1.10 Phenolphthalein $C_{12}H_8O_2$ (99%, Biochem), Sodium acetate $C_2H_3NaO_2$ (99.99%, Merck), Iron sulfate $FeSO_4{\cdot}7\ H_2O$ (>99, Merck), Potassium fluoride KF (98%, Fichersci), Hydrochloric acid HCl (37%, Sigma-Aldrich), Sulfuric acid H_2SO_4 (98%, Merck), Humic acid $C_9H_8Na_2O_4$ (>98%, Thermo Scientific), Chloroform $CHCl_3$ (Merck), Sodium sulfite Na_2SO_3 (98%, Sigma Aldrich), Potassium nitrate KNO_3 (>98%, Sigma Aldrich), and Potassium permanganate $KMnO_4$ (99%, Sigma Aldrich). Ultra-pure water was used to prepare solutions with high-purity. The dye is provided by an industrial food company, and a stock solution of initial SG dye concentration was prepared and used during all the experimental runs. A known concentration of H_2O_2 solution was prepared with distilled water by dilution of 30% *w/v* of stock solution and stored in amber-colored light-resistant glass bottles. All chemical substances are used without modification as received from the supplier.

2.2. Analytical methods

To determine the SG dye concentration of each sample throughout the photo-Fenton reaction time, a Shimadzu spectrophotometer analyzer (UV − 1800, Japan) at a maximum wavelength of λ = 520 nm was used and a HANNA pH meter is used to measure the pH levels of the solution.

In addition, the COD of samples at different operating conditions was also analyzed by the closed reflux titrimetric method to estimate the mineralization of SG dye [16]. The following formula (3 &nd 4)are used to calculate the dye removal yield by degradation and mineralization:

$$\mathbf{R}\% = \left(\frac{C_o - C_t}{C_o}\right)\mathbf{x\ 100} \quad (3)$$

Where;

C_o and C_t are the SG dye concentrations (mg/L) in the aqueous solutions before and after the reaction, respectively.

$$\mathbf{COD}\% = \left(\frac{COD_o - COD_t}{COD_o}\right)\mathbf{x\ 100} \quad (4)$$

Where;

COD_o and COD_t are the initial and at time (t) chemical oxygen

demand of liquid SG dye (mg O_2/ L), respectively.

2.3. Box-Benhken design

The Box-Behnken design (BBD), introduced by Box and Behnken in 1960, is a procedure to establish a statistical model within the framework of response surface methodology (RSM). This empirical model, in the form of a quadratic model, establishes a relationship between experimental factors and the resulting outcomes. Several studies, including those by Ferreira et al. in 2007, Witek-Krowiak et al. in 2014, and Sadhukhan et al. in 2016, have utilized BBD to analyze and interpret experimental data [17].

To determine the number of experiments (N) required for BBD, the following formula is employed: $N = 2\,K{\cdot}(K-1) + Co$. Here, K represents the number of factors, as discussed by Ferreira et al. in 2007 and Co signifies the number of repetitions of the center point. It is important to note that all factors are assigned three coded levels: low (−1), medium (0), and high (+1). To fit the experimental data to a second-order polynomial eq. (5) and identify the relevant model terms, a non-linear regression analysis is conducted.

$$Y = B_o + \sum_{i}^{k} B_i x_i + \sum_{i}^{k} B_{ii} x^2 + \sum_{ij}^{k} B_{ij} x_i x_j + E \tag{5}$$

In the above equation, Y represents the dependent variable, which denotes the SG uptake. The number of independent variables, or factors, is represented by k. Each independent variable is denoted by x_i, corresponding to its coded level. The regression coefficient at the center point is denoted as β_o, B_i represents the linear coefficient for the ith independent variable, B_{ii} represents the quadratic coefficients for the ith variable, and B_{ij} signifies the second-order interaction coefficient between the ith and the jth independent variables. The term E denotes the error component within the model. The works by Das and Das in 2014 and Shahbazi et al. in 2020 provide further insight into these variables and coefficients [17]. In order to examine the effect of independent parameters X_i and their interactions on a quantity of interest of the process Y (yield), called response on the rate of photodegradation in (%) and mineralization (%) of the SG dye and to optimize the operating conditions, the response surface methodology (RSM) was employed. Coded values of factors are usually used and the relationship between the actual values and the coded values is defined as:

$$x_i = \frac{X_i - X_0}{\Delta X_i} \tag{6}$$

Where X_i is the actual value of the ith variable; x_i is the coded value of X_i; X_o is the actual value of X_i at the center point, and ΔX_i is the step change [17].

In this study, the BBD technique was used for two distinct processes. In the first process, the efficiency of the complex (Fe(III)/Lig) for the degradation of food colorings was tested. For this purpose, three independent parameters were chosen and they are: the Fe(III) concentration (X_1), the molar ratio between ligand and iron (Lig/Fe(III)) (X_2), and the dye concentration (X_3). The second process was used to evaluate the efficiency of the complex (Fe(II)/Lig) in the degradation of food colorings. In this case, four independent factors were selected: X_1: the concentration of Fe(II), X_2: the molar ratio between the ligand and the iron (R = Lig/Fe(III)), X_3: the concentration of the dye and X_4: the H_2O_2 concentration. In both experimental designs, the rate of degradation (R %) and the yield of mineralization (COD%) were used as response variables (Y). Table 1 summarizes the factors with their delimited study ranges for the two processes. The intervals of each parameter were fixed after preliminary tests. The JMP program (JMP® Pro 13.0.0) was used to perform the statistical analysis.

In order to evaluate the efficiency of the BBD models of each output for the two processes, statistical criteria were used to evaluate the performance of the models with a confidence level of 95%. An analysis of variance (ANOVA) was conducted to determine the statistical capabilities of the generated models. Several variables and tools were considered to assess model fit, including probability (P-value), Fisher-test (F-value), Coefficient of Variance (C.V), Coefficient of Determination (R^2), Adjusted Coefficient of Determination (R^2_{adj}), and Root Mean Square Error (RMSE) for the BBD models [18–27]. The F value indicates the variation in responses, which can be assessed by a regression equation. Meanwhile, the P value determines the statistical significance of the developed models. A P value <5% is considered significant and the model fits the modified photo-Fenton reaction, while a P value >5% indicates model inadequacy [17,28–31].

Table 1
Factors and study area for both processes (Fe(III)/Lig) and (Fe(II)/Lig).

	Fe(III)/Lig			Fe(II)/Lig		
Level	−1	0	1	−1	0	1
X_1 (mM)	0.15	0.2	0.25	0.15	0.2	0.25
X_2 (Fe^{2+}/Oxy)	1	2	3	1	2	3
X_3 (mg/L)	10	15	20	10	15	20
X_4 (mM)				0.05	0.1	0.15

3. Results

3.1. Homogeneous photo-Fenton system

Before approaching the study of the removal of the SG dye in homogeneous modified photo-Fenton, operative information and conclusions are necessary to be obtained from the photodegradation study of the SG dye with a reference to the homogeneous system that uses dissolved iron.

3.2. Photo-Fenton evalution of possible reactions

It is known that the photo-Fenton reaction occurs with different reactive radicals such as OH*, O_2*, H_2O_2* HO_2* and iron (Fe(II), Fe(III)), meanwhile other reactions can occur simultaneously, and quickly inhibiting the photo-Fenton reaction [32].

In order to check possible undesirable parasitic reactions during the aforementioned processes, preliminary tests were carried out for SG dye with Fe(III), SG dye with Fe(II) and SG dye with a ligand. For this purpose, 20 mg/L of SG dye concentration was taken. The photolysis reaction experiment of the SG dye solution was also examined, followed by other tests in the dark in the presence of P/Fe(II), P/Lig and P/Fe(III). The results obtained are presented in terms of reduced concentration and are shown in Fig. 1.

The evolution of SG dye reduced concentration with time is shown in Fig. 1. It can be seen that the reduced concentration value for different reactions and transformation of the SG dye under sunlight irradiation remained constant during all the experiments. These results revealed that no reaction could take place and influence the photo-Fenton oxidation process of the SG dye [33]. Moreover, the fixed concentration of SG dye demonstrates high stability against the photolysis reaction and confirms their resistance to degradation in natural wastewater.

3.3. Influence of light sources nature

Light energy or irradiation is an important factor affecting water treatment efficiency. Thus, using a clean, sustainable energy and considering environmental and economic factors is crucial.

To better evaluate the contribution of the type of light sources in modified photo-Fenton oxidation mechanisms, UVA and LED as artificial light sources and sunlight as natural radiation were tested as excitation energy sources for both systems of photo-Fenton reaction Fe(III)/Lig and Fe(II)/Lig. The obtained results of the SG dye yield photo-Fenten degradation for different light sources are shown Fig. 2a and b.

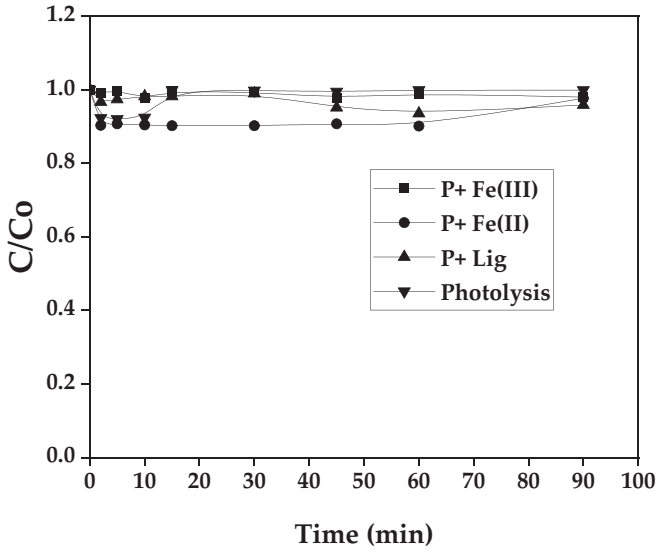

Fig. 1. Degradation rate of SG dye during photolysis and (P + Lig), (P+ Fe(II)) and (P + Fe(III)) without light. [P]o = 20 mg./L, [Lig]o = 0.3 mM, [Fe(II)]o = 0.1 mM, [Fe(III)]o = 0.1 mM.

From Fig. 2, it can clearly be observed that the rate of photo-Fenton degradation kinetics and the yield rate change from one light source to another. Regarding the process involving the complex of (Fe(III)/Lig) the UV light source has a 20% photo-Fenton degradation yield followed by 78% of LED light. However, the sunlight source gives interesting kinetics and a high yield record of 98%.

For other processes involving the complex (Fe(II)/Lig), we noticed the same trend in the (Fe(III)/Lig) system, with a marginal increase in the case of using UV light at the beginning of the reaction [34,35], the kinetics is faster than LED light but a degradation rate is 32%, for LED light the kinetics is slower at the beginning compared to UV light. After 1 h:30 min of reaction, the degradation yield under LED light is 50% becoming higher than that under UV light. The comparison of these results shows that sunlight is better and gives a very fast kinetics and a yield higher than 70%. This finding is a powerful motivation for encouraging to exploit sunlight source as a renewable energy during all our work for both (Fe(III)/Lig) and (Fe(II)/Lig) systems [35].

The primary factor contributing to the enhanced degradation and mineralization rate observed in sunlight-exposed experiments, as opposed to those irradiated with UV or visible light, can be attributed to the photoreduction of Fe(III)/complexes, resulting in the fast production of Fe(II) and *OH. Therefore, the generation of O_2^{*-} throughout several reactions from the O_2 present contributes in the yielding of degradation rate [14]. Additionally, the photodecarboxylation of Fe(III) by-product complexes formed during the degradation of SG also plays a role in this process. Moreover, Ferrioxalate is a photosensitive complex that is able to absorb light in wide solar spectrum range up to 550 nm with high quantum yield [13].

3.4. The BBD analysis

The main objective of the experimental design is to determine, with a minimum number of experiments, the effects of different parameters or factors Xi and their interactions on a process variable of interest *Y* (yield), called the response. In this work, the optimization of SG food dye degradation was performed on two complexes, namely (Fe(III)/Lig) and (Fe(II)/Lig), using the BBD approach. In both cases, the impacts of various factors, including the initial concentration of iron (0.15–0.25 mM), the molar ratio between the ligand and iron (1–3), and the dye concentration (10–20 mg/L), were investigated. In the case of the (Fe (II)/Lig) complex, an additional independent parameter, the H_2O_2 concentration (0.05–0.15 mM), was incorporated. Statistical analysis of the data was conducted using the JMP software (version 13 pro). The experimental trials' results, along with the corresponding experimental of the percentage of contribution of each factor and predicted values, are presented in Tables 2 and 3, where R% and COD% represent the rate of degradation and the rate of mineralization, respectively.

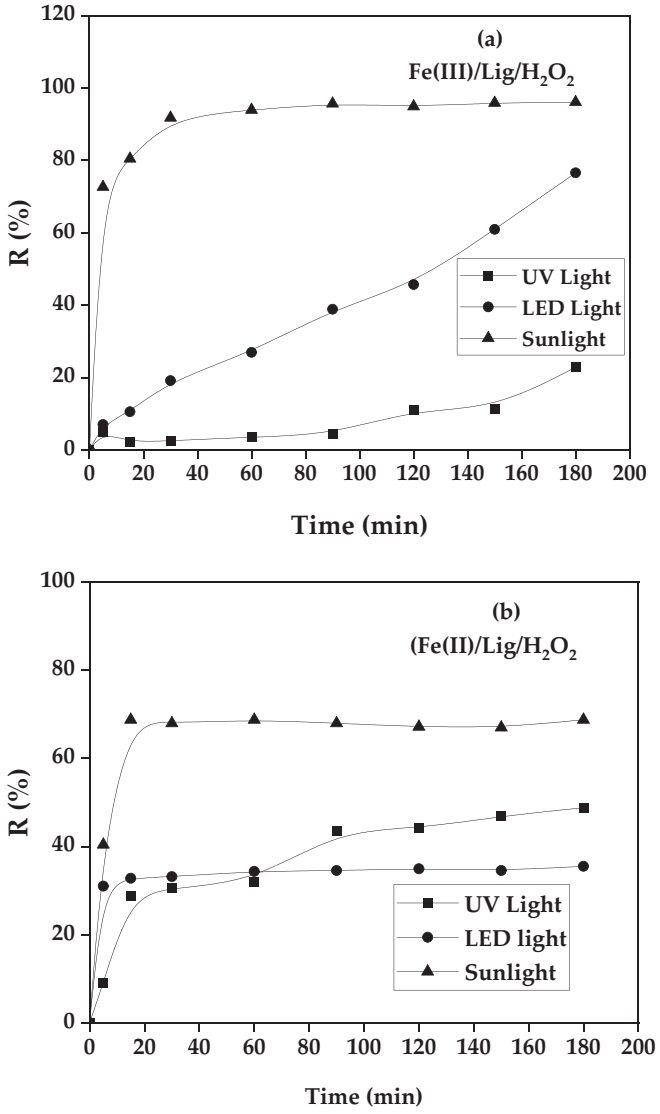

Fig. 2. Photo-Fenton degradation of SG under different light sources for a). Case of process (Fe(III)/Lig), b). Case of process (Fe(II)/Lig/H_2O_2) under experimental conditions [P]o = 10 mg. L^{-1}, [Fe(II)]o = 0.1 mM, [Fe(III)]o = 0.05 mM, *R* = 1, [H_2O_2]o = 0.1 mM.

The photo-Fenton process for the system (Fe(III)/Lig) shows a high percentage of response in terms of degradation or mineralization rate for all the three factors. The best results as optimization presented in Table 2 are 0.25 mM of Fe(III), molar ratio R = (Fe(III)/Oxydant) =2 and SG concentration 10 mg/L. In addition, Table 2 shows that the predicted values are close to those observed in all the experiments, for both degradation and mineralization.

The values of the SG degradation rate (R%) ranged from 77.95% to 99.64% and the values of mineralization (COD%) change from 72.89 to 98.02%, respectively as mentioned in Table 2 for the process Fe(II)/Lig and process Fe(III)/Lig.

Additionally, according to Table 3, the experimental values for the efficiencies of mineralization and degradation were 99.68% and 98.66%, respectively, whereas the corresponding predicted values were

101.80% and 99.23%, respectively.

The estimated equations consider the independent variables, their mutual interactions, and their quadratic influence are given by eqs. 7 and 8 for the (Fe(III)/Lig) and (Fe(II)/Lig) complexes, respectively.

$$Y = \beta_o + \beta_1 X_1 + \beta_2 X_2 + \beta_3 X_3 + \beta_4 X_1 X_2 + \beta_5 X_1 X_3 + \beta_6 X_2 X_3 + \beta_7 X_1^2 + \beta_8 X_2^2 + \beta_9 X_3^2 \quad (7)$$

$$Y = \beta_o + \beta_1 X_1 + \beta_2 X_2 + \beta_3 X_3 + \beta_4 X_4 + \beta_5 X_1 X_2 + \beta_6 X_1 X_3 + \beta_7 X_2 X_3 + \beta_8 X_1 X_4 + \beta_9 X_2 X_4 + \beta_{10} X_3 X_4 + \beta_{11} X_1^2 + \beta_{12} X_2^2 + \beta_{13} X_3^2 + \beta_{14} X_4^2 \quad (8)$$

Subsequently, the parameters with high explanatory power (PR < 5%) were selected and indicated in Table 4 with an asterisk symbol '*'. Conversely, the remaining parameters with PR > 5% were eliminated [17,28,30], and the models are represented by the equations provided in Table 5.

In the case of (Fe(III)/Lig) complex, the parameters that are not considered statistically significant (Prob >5%) are the interaction between X1 and X3, the quadratic effect of X1, and the quadratic effect of X3 in the dye degradation model (Table.4.1.1). In the COD model, the parameters X3, the interaction between X1 and X3, the quadratic effect of X1, and the quadratic effect of X3 are found to be non-significant (Table.4.1.2).

Meanwhile, in the (Fe(II)/Lig) complex, certain parameters are found to be statistically non-significant (Prob >5%). Specifically, in the R model, the non-significant parameters include the interaction between X1 and X3, the interaction between X2 and X3, and the interaction between X2 and X4 (Table.4.2.1). On the other hand, in the COD model, the non-significant parameters are X3 and X4, along with the following interactions: X1X3, X2X3, X1X4, X2X4, and X3*X4 (Table.4.2.2).

1. (Fe(III)/Lig)

$$DOC = 96.6733 + 2.6500 \times 1 + 6.4000 \times 2 - 4.8875\ X1X2 + 5.3525\ X2X3 - 6.9204\ X2X2 \quad (10)$$

Mineralization.

$$R = 97.6250 + 6.4080 \times 1 - 1.3973 \times 2 + 1.4647 \times 3 + 1.1710 \times 4 + 2.0140\ X1X2 - 3.8437\ X1X4 - 3.7187\ X3X4 - 5.2199\ X1X1 + 2.3751\ X2X2 - 3.9919\ X3X3 - 3.0849\ X4X4 \quad (11)$$

Mineralization.

$$DOC = 81.1800 + 1.2575 \times 1 + 6.2083 \times 2 + 1.3525\ X1X2 + 3.1229\ X1X1 + 6.1116\ X2X2 + 4.0204\ X3X3 + 2.0116\ X4X4 \quad (12)$$

2. (Fe(II)/Lig)

Photodegradation.

$$R = 97.1266 + 1.6350 \times 1 + 6.4837 \times 2 - 2.8587 \times 3 - 2.4075\ X1X2 + 3.3400\ X2X3 - 5.3283\ X2X2 \quad (9)$$

Photodegradation.

After eliminating the variables with low explanatory power, there was a slight decrease in the coefficients of determination, but the equation became more simplified.

The plotting of the experimental values against the predicted data derived from the model equation would also show if the regression models fit with the data. Fig. 3 shows a straight correlation line between the observed data and the model predictions with high agreement between them. As a result, we may say that the quadratic polynomial model accurately depicts the relationship between the predictor and response variables. Moreover, these coefficients indicate moderately positive correlations within the model (Fig. 3). The probability was determined to be strictly below 0.5%, confirming that the model is extremely significant. Additionally, the significance level of *P*-value and F Ratio values, which assess the statistical significance of the regression

Table 2
Experimental and predicted response for SG degradation and mineralization under Box-Benhken design with (Fe(III)/Lig) complex.

N	X_1	X_2	X_3	R%	Predicted R%	COD%	Predicted COD%
1	−1	0	1	93.63	91.77	90.92	90.88
2	−1	0	−1	98.75	99.44	95.83	96.45
3	0	1	−1	99.47	101.13	94.17	98.05
4	0	1	1	98.25	98.05	97.33	92.96
5	0	0	0	97.25	81.32	96.00	74.23
6	1	0	−1	99.64	89.41	95.50	89.31
7	0	0	0	97.25	97.13	96.00	96.67
8	−1	−1	0	81.25	97.13	72.89	96.67
9	0	−1	−1	92.53	97.13	92.83	96.67
10	1	0	1	97.69	99.10	98.00	96.81
11	0	0	0	96.88	97.56	98.02	92.33
12	1	−1	0	90.13	79.37	89.89	75.79
13	−1	1	0	98.38	92.14	96.22	88.37
14	0	−1	1	77.95	96.99	74.58	97.38
15	1	1	0	97.63	99.06	93.67	99.29

Table 3
Experimental and predicted response for SG degradation and mineralization under Box–Benhken design of experiments for the process Fer(II)/Lig.

N	X_1	X_2	X_3	X_4	R%	Predicted R%	COD %	Predicted COD %
1	−1	−1	0	0	93.37	91.78	84.66	84.30
2	−1	0	−1	0	81.88	82.13	87.33	86.316
3	−1	0	0	−1	76.63	77.89	85.33	85.10
4	−1	0	0	1	88.75	87.93	85.33	85.01
5	−1	0	1	0	80.5	81.87	86.66	87.82
6	−1	1	0	0	85.46	84.96	93.25	94.03
7	0	−1	−1	0	96.35	96.55	84	84.02
8	0	−1	0	−1	97.5	96.04	84	84.21
9	0	−1	0	1	99.12	100.59	81.16	81.98
10	0	−1	1	0	97.92	98.26	86.33	86.18
11	0	0	−1	−1	82.88	84.19	87.33	88.70
12	0	0	−1	1	93.5	93.97	84.88	85.72
13	0	0	0	0	97.63	97.63	81.33	81.18
14	0	0	0	0	97.63	97.63	79.88	81.18
15	0	0	0	0	97.63	97.63	82.33	81.18
16	0	0	1	−1	94.5	94.56	87.44	86.81
17	0	0	1	1	90.25	89.47	88.77	87.61
18	0	1	−1	0	93.43	92.54	99.16	98.60
19	0	1	0	-1	96.92	95.45	95.83	95.49
20	0	1	0	1	94.10	95.58	95.25	95.53
21	0	1	1	0	97.43	96.68	97.16	96.44
22	1	-1	0	0	99.54	100.57	84.66	84.11
23	1	0	-1	0	93.13	91.76	91	90.33
24	1	0	0	-1	98.13	98.40	89	88.63
25	1	0	0	1	94.88	93.06	87	86.53
26	1	0	1	0	98.13	97.88	87.33	88.83
27	1	1	0	0	99.67	101.80	98.66	99.23

models, were calculated. A high F value coupled with a low P-value indicates the statistical significance of the model [36].

The significance of the determination coefficient (R^2) comes in its ability to indicate the level of adequacy of a generated model, as it corresponds to the ratio of the explained variation by the model to the overall variance [37]. Moreover, the adequacy of the model in accurately representing the experimental data may be determined by assessing the proximity of the R^2 value to the unity, as stated by Garba et al. (2014) [38]. It is observed that the R^2 values for eq. 7, and eq. 8 were higher than 0.96, as shown in Table 5. These findings suggested that the experimental factors examined account for about 96% of the degradation and mineralization rate of the SG dye. The R^2 coefficient values demonstrate a strong and satisfactory level of concordance with the modified R^2 values, hence substantiating the statistical significance of the model.

The developed models through BBD have the capability to analyze the influence of predictors, their interactions, and their terms on the response variable simultaneously as presented in Table 4. Notably, the coefficients assigned to the individual factors within the model enable the assessment of their individual impact on the response.

3.5. Response surface analysis

The BBD was used to study the effect of the operating parameters for each complex on food dye degradation [39]. Response surface analysis is a set of mathematical and statistical techniques for improving and optimizing processes through the use of a large number of designed experiments [40]. Response surface analysis is a useful way to determine the effects, to investigate the relationship between multiple variables and the selected response variable. The individual effects and interactions of the predictor variables of each process are discussed below.

3.5.1. Effect of parameters on R%

3.5.1.1. Complex (Fe(III)/Lig). In the context of complex (Fe(III)/Lig) analysis for SG dye degradation (R model), the results can be interpreted based on the following points. Each parameter corresponds to a βi value given in Table 4. Generally, where a negative βi value indicates a negative effect of such parameter on the SG degradation and represents an antagonistic effect. Thus, when the parameter increases, the degradation rate decreases, and conversely, when the parameter decreases, the degradation rate increases. On the other hand, a positive value of βi indicating their positive effect of the parameter on the SG degradation rate and represents a synergistic effect. Also, this means that when the parameter increases, the degradation rate also increases, and when the parameter decreases, the rate efficiency of degradation decreases. First, the probability values (Prob) must be taken into account to assess the significance of the parameters. When the value of Prob is >0.05, this indicates a non-significant effect of the parameter on SG dye removal degradation. On the other hand, when the value of Prob is <0.05, this confirms that the parameter is statistically significant.

On the basis of static data, this study demonstrates that the significant parameters influencing the elimination of SG by photo-Fenton degradation using the (Fe(III)/Lig) complex are X1 (Fe(III) concentration), X2 (ratio = Lig/Fe(III)), X3 (P: SG dye concentration), X1X2 (the interaction between X1 and X2), X2X3 (the interaction between X2 and X3) and X2^2 (the quadratic effect of X2) (Table 4). These parameters exert a significant positive effects on SG degradation. It is important to note that the other parameters are not considered significant in this model, which suggests that they do not have a major influence on the degradation of the SG dye.

For the degradation rate, by examining the specific results of the significant parameters, it is observed that some parameters had positive "βi" values (Table 4), which revealed a significant and positive effect on SG degradation rate. The parameters X1 and X2 present a βi values of

Table 4
Model parameters and analysis of the BBD models for the two complexes.

i	Term	βi	Std Error	t Ratio	Prob > |t|	βi	Std Error	t Ratio	Prob > |t|
Response		a. R%				b. COD%			
	Complex				1. (Fe(III)/Lig)				
0	Intercept	97.1266	0.8844	109.8200	<0.0001*	96.6733	1.4461	66.8500	<0.0001*
1	X1	1.6350	0.5416	3.0200	0.0295*	2.6500	0.8855	2.9900	0.0304*
2	X2	6.4837	0.5416	11.9700	<0.0001*	6.4000	0.8855	7.2300	0.0008*
3	X3	−2.8587	0.5416	−5.2800	0.0032*	−2.1875	0.8855	−2.4700	0.0565
4	X1*X2	−2.4075	0.7659	−3.1400	0.0256*	−4.8875	1.2523	−3.9000	0.0114*
5	X1*X3	0.7925	0.7659	1.0300	0.3482	1.8525	1.2523	1.4800	0.1992
6	X2*X3	3.3400	0.7659	4.3600	0.0073*	5.3525	1.2523	4.2700	0.0079*
7	X1*X1	0.0491	0.7972	0.0600	0.9532	−1.5854	1.3035	−1.2200	0.2782
8	X2*X2	−5.3283	0.7972	−6.6800	0.0011*	−6.9204	1.3035	−5.3100	0.0032*
9	X3*X3	0.2516	0.7972	0.3200	0.7650	−0.0254	1.3035	−0.0200	0.9852
	Complex				2. (Fe(II)/Lig)				
0	Intercept	97.6250	0.9221	105.8700	<0.0001*	81.1800	0.6679	121.5500	<0.0001*
1	X1	6.4080	0.4610	13.9000	<0.0001*	1.2575	0.3339	3.7700	0.0027*
2	X2	−1.3973	0.4610	−3.0300	0.0105*	6.2083	0.3339	18.5900	<0.0001*
3	X3	1.4474	0.4610	3.1800	0.0080*	−0.0008	0.3339	−0.0000	0.9980
4	X4	1.1710	0.4610	2.5400	0.0259*	−0.5450	0.3339	−1.6300	0.1286
5	X1*X2	2.0140	0.7985	2.5200	0.0268*	1.3525	0.5784	2.3400	0.0375*
6	X1*X3	1.5937	0.7985	2.0000	0.0692	−0.7500	0.5784	−1.3000	0.2191
7	X2*X3	0.6057	0.7985	0.7600	0.4628	−1.0825	0.5784	−1.8700	0.0858
8	X1*X4	−3.8437	0.7985	−4.8100	0.0004*	−0.5000	0.5784	−0.8600	0.4043
9	X2*X4	−1.1069	0.7985	−1.3900	0.1909	0.5650	0.5784	0.9800	0.3479
10	X3*X4	−3.7187	0.7985	−4.6600	0.0006*	0.9450	0.5784	1.6300	0.1283
11	X1*X1	−5.2199	0.6916	−7.5500	<0.0001*	3.1229	0.5009	6.2300	<0.0001*
12	X2*X2	2.3751	0.6916	3.4300	0.0049*	6.1116	0.5009	12.2000	<0.0001*
13	X3*X3	−3.9919	0.6916	−5.7700	<0.0001*	4.0204	0.5009	8.0300	<0.0001*
14	X4*X4	−3.0849	0.6916	−4.4600	0.0008*	2.0116	0.5009	4.0200	0.0017*

1.635 and 6.48375 (Table 4), respectively, suggesting that an increase in X1 (Fe(III)) and X2 of Lig/Fe(III) would lead to an increase in the SG degradation rate (Fig. 4a).

On the other hand, some parameters have negative βi values, which means that they had a negative effect on the SG degradation. For example, the parameter X3 corresponding to SG concentration has a βi value of −2.85875 (Table 4), implying that an increase in X3 would lead to a decrease in the rate of SG dye degradation (Fig. 4b). Moreover, the interaction between X1 and X2 (parameter X1X2) shows a βi value of −2.4075 (Table 4), indicating a strong negative effect on the degradation of the dye (Fig. 4a). It is important to note that the interaction between X2 and X3 (parameter X2X3) also has a significant positive effect (Fig. 4b), with a βi value of 3.34 (Table 4).

From the obtained result shown in Table 4, the quadratic effect of X2 (the parameter X2^2) was also observed through a βi value of −5.328333 (Table 4). This negative value indicates the adverse effect of this variable on the degradation process (Figs. 4a and b). As X2 increases, the rate of dye degradation decreases, Meanwhile, a further increase of X2, the SG rate degradation begins to increase again. This may indicate a synergistic effect and an optimal point where X2 has the greatest impact on SG dye degradation.

It may be concluded from this study which highlights several important parameters in the degradation of the SG dye with the complex (Fe(III)/Lig) had a significant positive effect among them X1, X2, X3 and X2^2.

3.5.1.2. Complex (Fe(II)/Lig). This part evaluates the surface responses analysis in the case of (Fe(II)/Lig) complex used for the SG dye rate degradation (R model) on the photo-Fenton process to evaluate the significance of potential interactions between independent variables and model responses, to determine the significance of the effect of each independent variable based on the F values and the probability of accuracy of the results with prob. > F. From Table 4, the parameters with Prob results <0.05 demonstrate significant parameters influencing SG degradation rate. Among the significant parameters are X1 (Fe(II) Concentration), X2 (ratio = Lig/Fe(II)), X3 (P SG dye Concentration), X4 (H_2O_2 Concentration), the interaction between X1 and X2 (X1X2), the interaction between X1 and X4 (X1X4), the interaction between X3 and X4 (X3X4), the quadratic effect of X1 (X1X1), the quadratic effect of X2 (X2X2), the quadratic effect of X3 (X3X3) and the quadratic effect of X4 (X4*X4) (Table 4). These parameters exert significant effects on SG degradation rate, whether positive or negative. The effect of each parameter can be evaluated by referring to the corresponding βi values (Table 4).

Table 4 shows that X1 has a βi value of 6.4080218, suggesting that an increase in X1 would lead to enhancing the SG degradation rate (Fig. 5a

Table 5
The final BBD model equations and performance measures for photo-Fenton degradation and mineralization by (Fe(III)/Lig) and (Fe(II)/Lig) complex.

Responses	Final equation in terms of code of independent variables	P	F	R^2	RMSE
	(Fe(III)/Lig)				
R%	$Y_1 = \beta_0 + \beta_1X_1 + \beta_2X_2 + \beta_3X_3 + \beta_4X_1X_2 + \beta_6X_2X_3 + \beta_8X_2^2$	0.0116*	8.0415	0.98	1.5319
COD %	$Y_2 = \beta_0 + \beta_1X_1 + \beta_2X_2 + \beta_4X_1X_2 + \beta_6X_2X_3 + \beta_8X_2^2$	0.01272	7.0211	0.96	2.5848
	(Fe(II)/Lig)				
R%	$Y_1 = \beta_0 + \beta_1X_1 + \beta_2X_2 + \beta_3X_3 + \beta_4X_4 + \beta_5X_1X_2 + \beta_8X_1X_4 + \beta_{10}X_3X_4 + \beta_{11}X_1^2 + \beta_{12}X_2^2 + \beta_{13}X_3^2 + \beta_{14}X_4^2$	0.001*	3.06125	0.97	1.5972
COD%	$Y = \beta_0 + \beta_1X_1 + \beta_2X_2 + \beta_5X_1X_2 + \beta_{11}X_1^2 + \beta_{12}X_2^2 + \beta_{13}X_3^2 + \beta_{14}X_4^2$	0.0491*	0.8583	0.98	1.1568

and b). Similar tendence have been observed for X3 and X4, which exhibit a βi values of 1.4647436 and 1.1710871, respectively (Table 4), confirming its strong positive effect on dye degradation (Fig. 5c).

On the other hand, the parameters exhbit negative βi values of −1.397363 such as X2 (Table 4), which means that they have a negative effect on dye degradation and implying that an increase in X2 would lead to a decrease in the degradation rate of SG dye (Fig. 5a). Moreover, the interaction between X1 and X4 (X1*X4) has a significant negative effect (Fig. 5b), with a βi value of −3.84375 (Table 4).

Furthermore, the interactions X1X2 and X3X4 and the quadratic effects of X1X1, X2X2, X3X3 and X4X4 are also statistically significant. The interaction between X1 and X2 (X1X2) and between X3 and X4 (X3X4) have a βi values of 2.0140452 and 1.59375, respectively (Table 4), indicating a significant positive effect of this interaction on SG degradation reaction (Fig. 5a, c). Meanwhile, the interaction between X1 and X4 (X1*X4) has a significant negative effect (Fig. 5b), with βi value of −3.84375 (Table 4).

The quadratic effect of X1 (X1X1) and X3 (X3X3) have a value of βi of −5.219975 and − 3.084979, respectively (Table 4), suggesting a nonlinear relationship between X1, X3 and the SG degradation rate (Fig. 5a,5b and 5c). Also, this finding denoting that there is an optimal value of X3 to maximize the degradation rate. Similarly, the quadratic effect of X2 (X2X2) displays a βi value of 2.3751778 (Table 4), due to this fact it's indicating a nonlinear relationship between X2 and SG degradation rate (Fig. 5a). Finally, the quadratic effect of X4 (X4X4) shows a value of βi of −3.084979 (Table 4), also demonstrating a nonlinear relationship between X4 and SG degradation rate (Fig. 5b and c). Consequently, this was evidence to note that this quadratic effect inhibited the degradation rate of SG.

In summary, the present examination of the recently obtained data revealed the importance and the significance of certain factors in the degradation rate of SG dye for the system of (Fe(II)/Lig) complex.

3.5.2. *Effect of parameters on COD %*

3.5.2.1. Complex (Fe(III)/Lig). The response surface methodology was applied to reveal the effect of the independent variables and the interaction between them with aim to predict the SG mineralization rate COD % (COD model) in the case of using the complex (Fe(III)/Lig), the variables considered are Fe(III) concentration (X1), molar ratio Lig/Fe(III) (X2) and SG dye concentration (X3). The analysis was conducted by preparing 3D response surface plot and the normal of probability "Prob" revealed the satisfactory with the significance of parameters that impact the SG mineralization rate. The obtained results indicated that the level

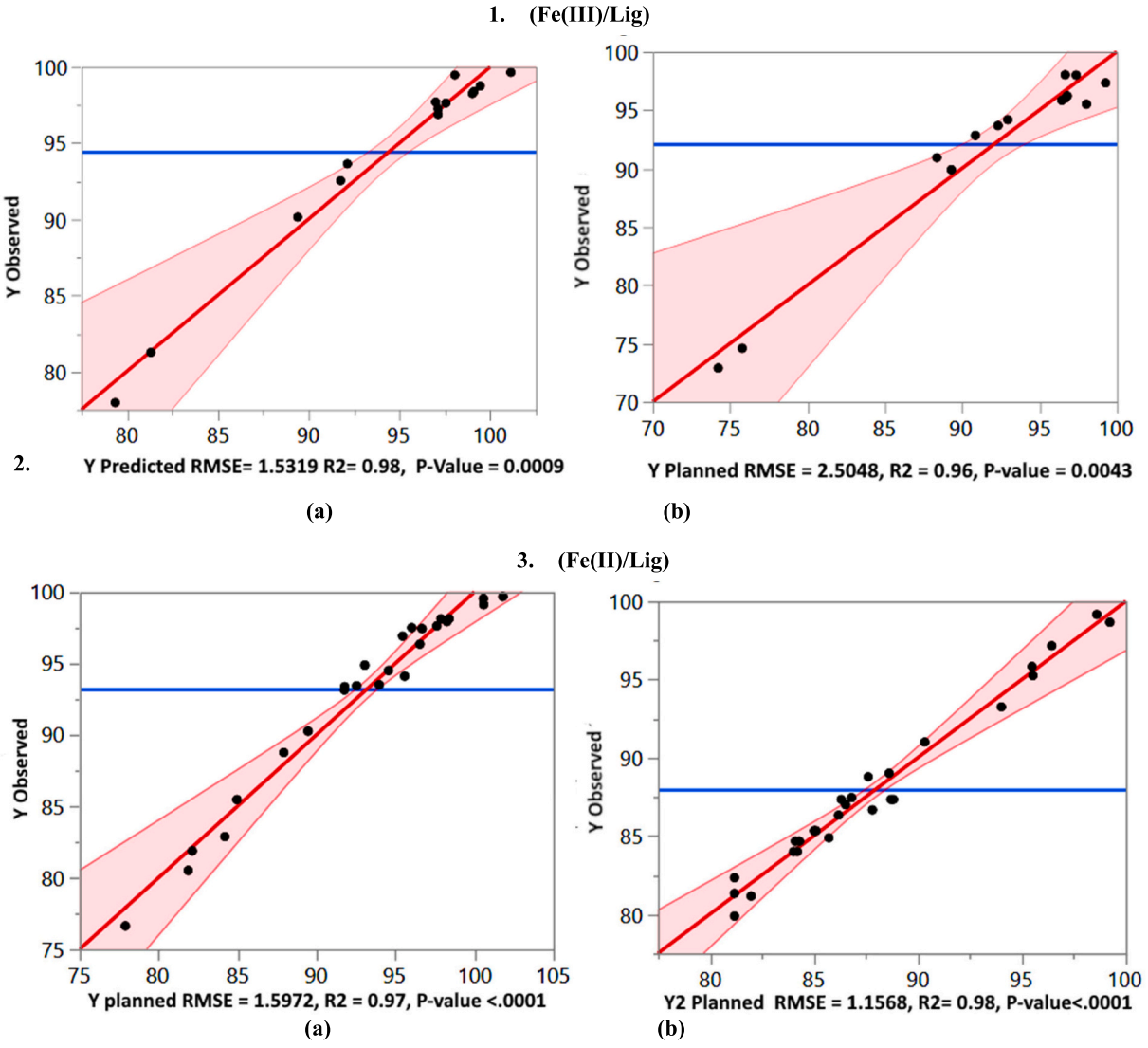

Fig. 3. Relation between the observed values and those estimated by the BBD models For (Fe(III)/Lig) and (Fe(II)/Lig) complexes: (a) R% degradation and (b) COD % mineralization.

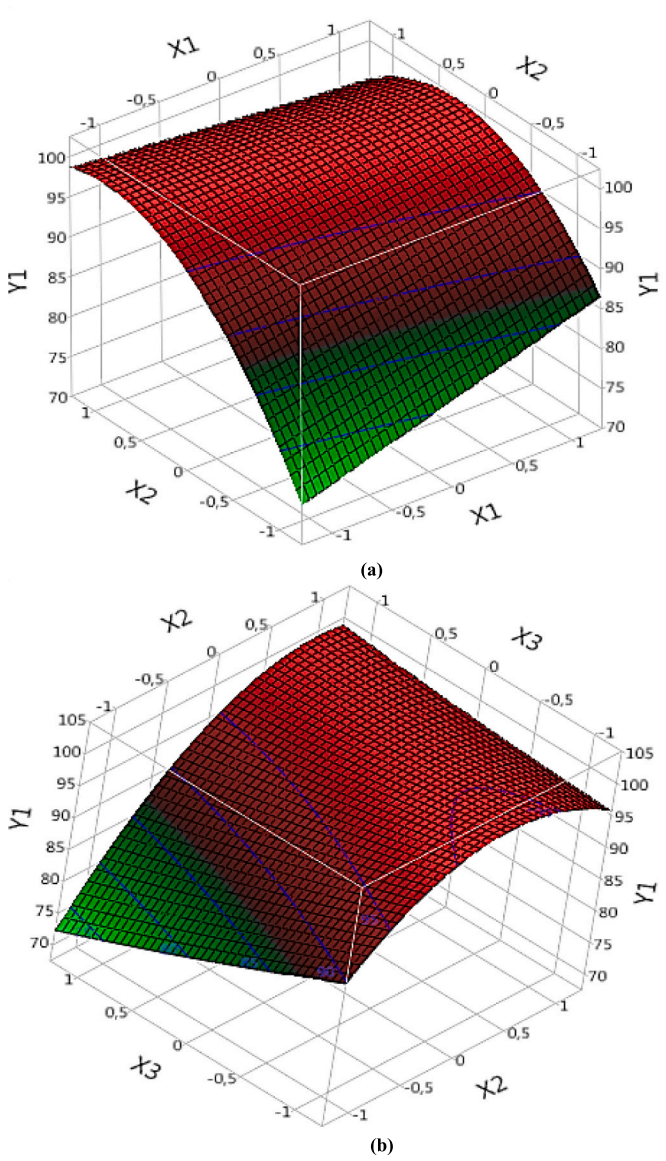

Fig. 4. Effects of operating factors and their interactions on the SG degradation rate by the (Fe(III)/Lig) complex: a) interaction between X1 and X2 and b) interaction between X2 and X3.

of statistical significance of parameters including: X1, X2, the interaction between X1 and X2 (X1X2), the interaction between X2 and X3 (X2X3), and the quadratic effect of X2 (X2X2) (Table 4). Therefore, these parameters exert significant effects on SG mineralization rate, whether positive or negative. The effect of each parameter can be evaluated by referring to the corresponding "βi" value (Table 4).

By examining the specific results of the significant parameters, it is observed that certain parameters have positive "βi" values, indicating a significant factors and positive effect on the SG rate of mineralization. For example, X1 and X2 have a "βi" values of 2.65 and 6.4 (Table 4), suggesting that this parameters are promoting factor in the process of photo-Fenton, an increase in X1 and X2 would lead to enhanced the SG mineralization rate (Fig. 6a) confirming its significant positive effect on dye mineralization (Fig. 6a and b).

It should be mentioned that the interactions between the parameters X1X2 and X2X3 are also significant. The interaction between X1 and X2 (X1X2) and X2 (X2X2) have a "βi" value of −4.8875 and − 6.920417 (Table 4), demonstrating a significant effect of this interaction in SG mineralization rate (Fig. 6a) and suggesting a non-linear relationship between X2 and SG mineralization rate (Fig. 6a and b), the interaction between X2 and X3 (X2X3) presents a "βi" value of 5.3525 (Table 4), confirming its significant effect on the SG mineralization rate (Fig. 6b).

Then, the quadratic effect of X2 (X2X2) is also significant, it gives a "βi" value of −6.920417 (Table 4), this result. It is important to note that

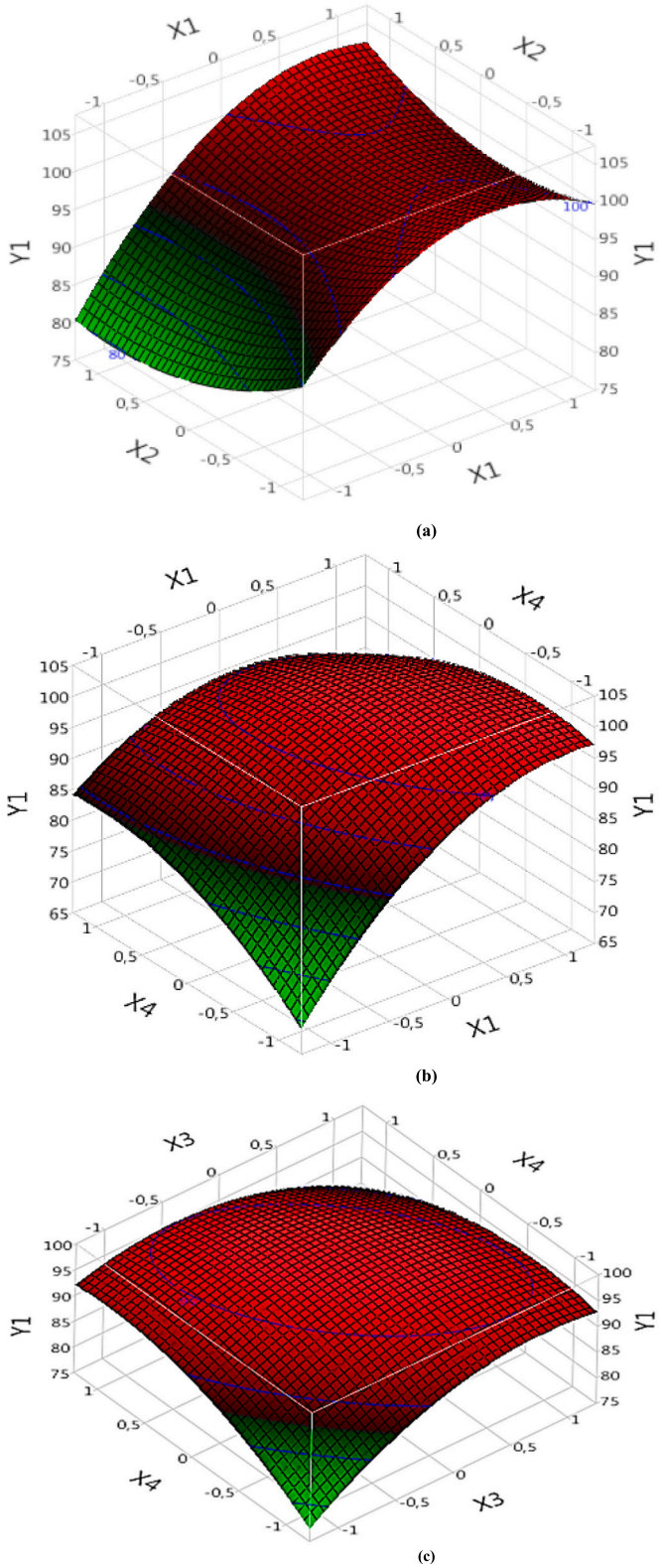

Fig. 5. Effects of operating factors and their interactions on the degradation of the dye under Complex (Fe(II)/Lig): a) interaction between X1 and X2, b) interaction between X1 and X4, and c) interaction between X3 and X4.

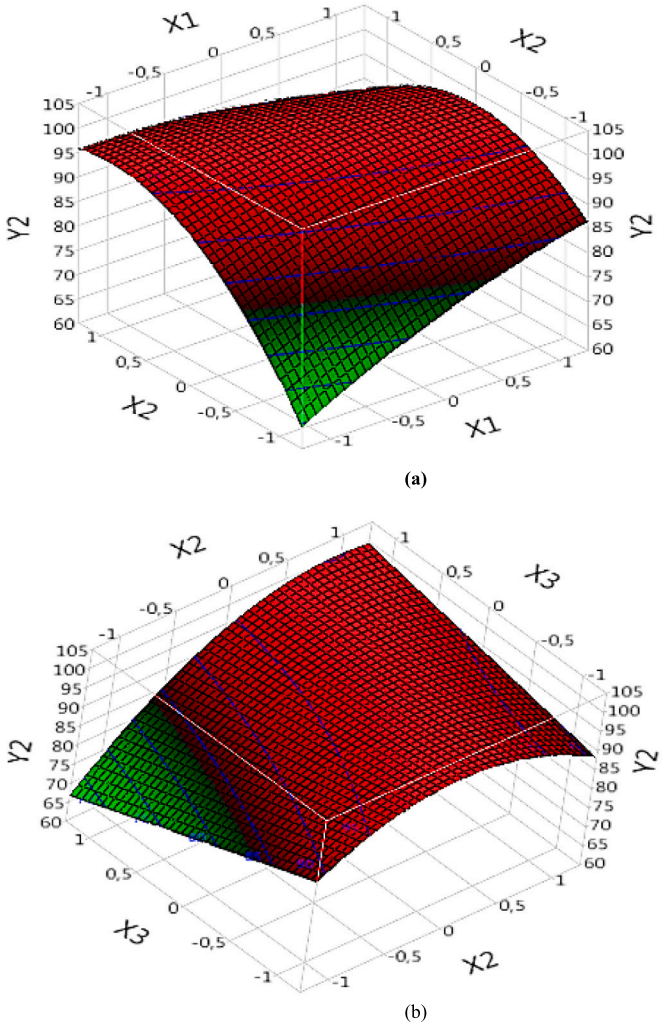

Fig. 6. Effects of operating factors and their interactions on the mineralization of the SG dye under Complex (Fe(III)/Lig): a) interaction between X1 and X2, and b) interaction between X2 and X3.

this quadratic effect has a negative impact on the SG of mineralization rate.

Finally, the analysis performed with response surface methodology for the reaction of mineralization of SG dye by the complex (Fe(III)/Lig), indicated its suitable analyzing the effect of various variables and confirmed the role of some factors in improving the SG mineralization.

3.5.2.2. Complex (Fe(II)/Lig). The study of surface response modeling of the SG mineralization reaction with the complex (Fe(II)/Lig) (COD model), this technique was used to study and optimize the SG photo-Fenton degradation processes under sunlight irradiation. Therfore, the use of probability "Prob" value for comparing the significant parameters that could be influence positively or negatively the SG mineralization rate.

The analysis of results showed that the significant parameters include X1, X2, the interaction between X1 and X2 (X1X2), the quadratic effect of X1 (X1X1), the quadratic effect of X2 (X2X2), the quadratic effect of X3 (X3X3) and the quadratic effect of X4 (X4X4) (Table 4). In addition, these parameters play significant effects on SG mineralization rate, whether positive or negative. The effect of each parameter can be evaluated by referring to the corresponding "βi" values (Table 4).

Furthermore, X1, X2 exhbit a "βi" values of 1.2575 and 6.2083333, respectively (Table 4), suggesting that an increase in X1 and X2 would lead to an increase in the SG rate of mineralization (Fig. 7a) this

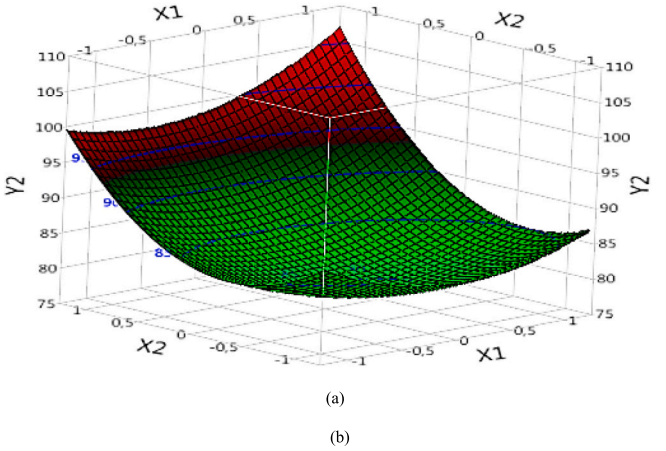

Fig. 7. Effects of operating factors and their interactions on the mineralization of the SG dye under Complex (Fe(II)/Lig): a) interaction between X1 and X2, and b) interaction between X3 and X4.

confirming its significant positive effect on the SG mineralization rate (Fig. 7a).

Also, it may be noticed, another significant effect, with a value of "βi" of 1.3525 (Table 4) for the interaction between X1 and X2 (X1X2) suggested that this interaction is associated with a positive effect on SG mineralization (Fig. 7a), and a simultaneous increase in X1 and X2 will further favours the mineralization rate of SG.

Next, the SG mineralization (Fig. 7a), the quadratic effects of X1 (X1X1), X2 (X2X2), X3 (X3X3) and X4 (X4X4) are also significant. For example, the quadratic effect of X1 (X1X1) had a "βi" value of 3.1229167 indicated a nonlinear relationship between the varaibles X1 and SG mineralization rate. Likewise, the quadratic effect of X2 (X2X2) exhibits a "βi" value of 6.1116667 (Table 4), also revealed a non-linear relationship between X2 and the SG mineralization rate (Fig. 7a). Similar, the quadratic effects of X3 (X3X3) and X4 (X4X4) also have significant values (Fig. 7b), with "βi" values of 4.0204167 and 2.0116667, respectively (Table 4).

Finally, the data analysis with surface response methodology for the modified homogeneous photo-Fenton mineralization reaction of SG dye by the complex (Fe(II)/Lig), demonstrated their validity, suitability and determined the significant parameters with positive effect and those with negative effect on the mineralization reaction.

3.6. Multi-objective optimization and validation

In this study, two primary objectives were defined for the optimization process. The first objective, labeled "Removal Efficiency," measures the percentage of SG dye removed through the photo-Fenton process. The second objective, named "Chemical Oxygen Demand Reduction," quantifies the percentage reduction in chemical oxygen demand, which serves as an indicator of the degradation of organic

Table 6
The obtained optimum conditions and experimental validation.

	R (%)	COD (%)	(R (%) + COD (%))/2
(Fe(III)/Lig)			
• X1 = 0.15 mM, X2 = 3, and X3 = 20 mg/L			
Experimental	98.73	99.87	99.30
Predicted response	99.53	103.74	101.63
Error	0.8	3.87	2.33
(Fe(II)/Lig)			
• X1 = 0.25 mM, X2 = 3, and X3 = 20 mg/L and X4 = 0.05 mM			
Experimental	99.63	99.92	99.77
Predicted response	102.58	105.26	103.92
Error	2.95	5.34	4.14

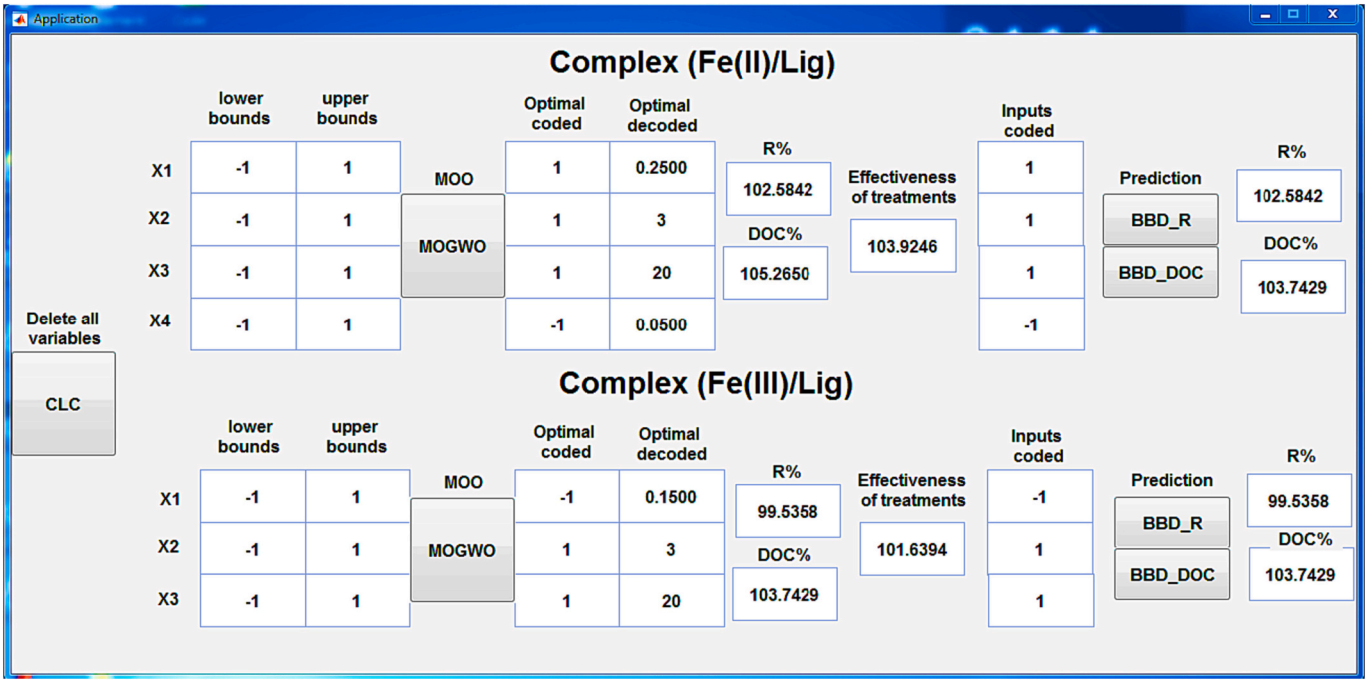

Fig. 8. Application based on an interface of MATLAB for MOO (MOGWO), and prediction R%, COD % and processing efficiency using BBD by the two complexes.

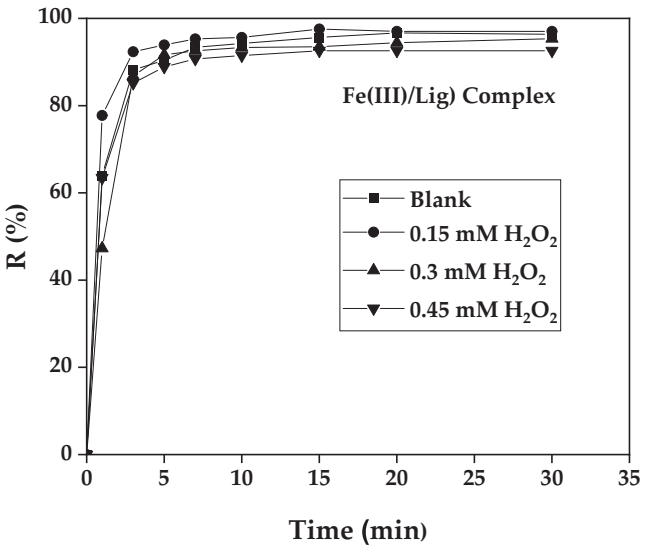

Fig. 9. Influence of H_2O_2 concentration on SG dye photo-Fenton degradation, [p]o = 10 mg/L^{-1}, Fe(III) = 0.15 mM, R = 2 and pHi not adjusted.

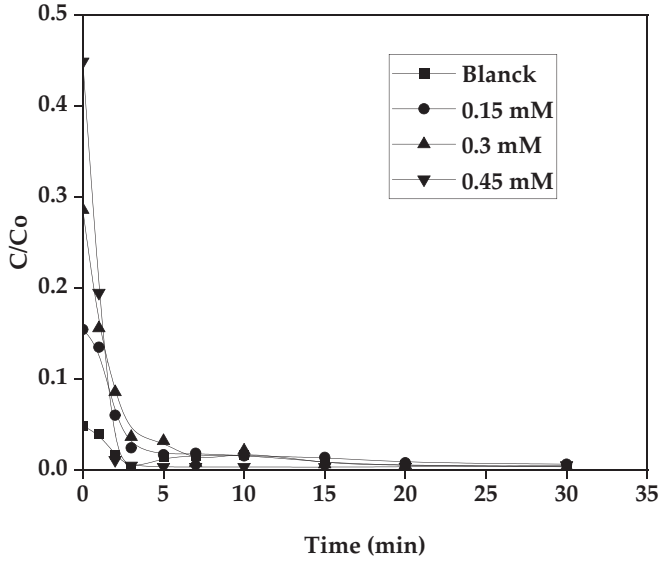

Fig. 10. Production and consumption of H_2O_2 during the degradation of the SG pollutant, [P]o = 10 mg/L^{-1}, Fe(III) = 0.15 mM and R = 2.

pollutants in water. Both objectives were considered equally important, each receiving a weighting of 50% in the optimization process. Thus, the weighted sum of these objectives was used as a single guiding objective.

To determine the optimal parameters for the (Fe(II)/Lig) and (Fe (III)/Lig) complexes in the context of SG dye removal via homogeneous photo-Fenton reaction, a specific optimization method was employed. This method is known as "Multi-Objective Grey Wolf Optimizer" (MOGWO). MOGWO is an extension of the Grey Wolf Optimizer (GWO) algorithm tailored for solving optimization problems with multiple objectives [28,29,39]. Its primary aim is to find a set of efficient solutions known as "Pareto-optimal solutions," which represent trade-offs between the different objectives. To achieve this, MOGWO employs search mechanisms inspired by the hunting behavior and social hierarchy of grey wolves. It explores the solution space to converge towards the Pareto front, where optimal solutions balancing the objectives are found [40,41]. What sets MOGWO apart is its ability to provide a diverse array of solutions within the objective space, offering decision-makers a range of options for decision-making. It also utilizes operators such as alpha, beta, and delta wolf movements to navigate the search space and select non-dominated solutions.

A critical step following the acquisition of optimal parameter values through MOGWO was laboratory validation. This validation phase had two primary objectives. First, it aimed to confirm the efficiency and accuracy of the models obtained during the optimization, thus ensuring the relevance of theoretical results in practical settings. Additionally, the validation step played a crucial role in selecting the most effective complex among the available choices (Fe(II)/Lig or Fe(III)/Lig) for use in the SG dye removal process via the photo-Fenton reaction. It,

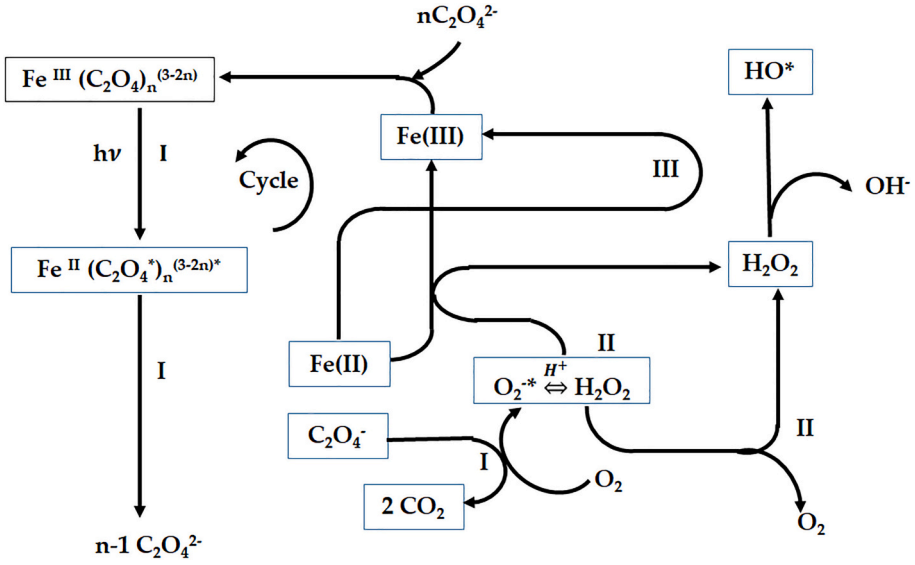

Fig. 11. Scheme of the cycle of the Fe(III)-oxalate complex under the effect of light with the formation of H_2O_2 [43].

therefore, had a significant impact on decision-making for the real-world application of the process.

The obtained optimal parameter settings are given in Table 6, where their experimental validation results are also given. The experimental validation results show an exceptional degradation and mineralization case of the SG contaminant for both complexes, resulting in nearly perfect treatment efficiency (almost 100%). Furthermore, the obtained error was around 5%, affirming the effectiveness and robustness of the models developed through BBD. These findings underscore the remarkable performance and reliability of the optimized conditions, reinforcing their potential for successful implementation in real-industrial settings.

3.7. *Interface for optimization and prediction*

In pursuit of delivering a practical solution for the implementation of multi-objective optimization (MOO) and the prediction of key parameters such as R%, COD%, and processing efficiency for various complexes, we have developed a user-friendly interface utilizing MATLAB's guide framework. This interface, as illustrated in Fig. 8, has been further transformed into an executable application tailored for the Windows operating system. This versatile application presents a valuable and accessible means to forecast outcomes by allowing users to select input values corresponding to the specific type of complex defined by the BBD. It empowers users to discover a MOO solution by identifying the optimal input values for each complex, achieved through the utilization of the MOGWO algorithm. By virtue of this application, individuals seeking to anticipate results and fine-tune parameters for each complex can now do so in a highly customized manner, tailored to their distinct requirements. The user-friendly interface simplifies the process, enabling users to obtain precise predictions and determine optimal parameters. This capability is invaluable for informed decision-making concerning

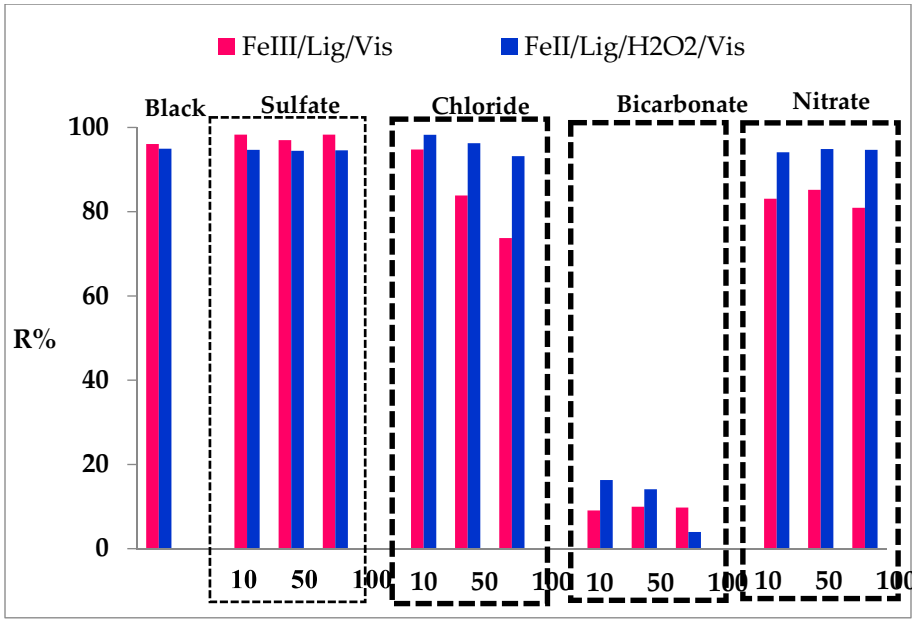

Fig. 12. Effect of inorganic ions intervening the two complexes (Fe(III)/Lig) and (Fe(II)/Lig). [P]o = 10 mg/L, [Fe(II)]o = [Fe(III)]o = 0.2 mM, $R = 2$, $[H_2O_2]o$ = 0.15 mM and for 30 min.

the degradation of dyes, offering practical solutions and insights for a wide range of applications.

3.8. nfluence of H_2O_2 concentration

To better understand the effect of the initial concentration of H_2O_2 on the kinetics of photo-Fenton oxidation of the SG dye degradation or mineralization, the production, as well as the consumption of hydrogen peroxide, were carried out according to different initial concentrations of H_2O_2 (0,15–0.3 and 0.45 mM.) while keeping the initial concentrations of SG and Fe(III) constant at free pH. All these results obtained are represented in Figs. 9 and 10.

From the results depicted in Fig. 9, it was observed that for a concentration of 0.15 mM a slightly fast kinetics occurred, with a similar yield of discoloration with the control reaction. However, for concentrations of 0.3 mM and 0.45 mM H_2O_2, it was noted that the yield decreased slightly when the degradation kinetics became slow, this indicated that above the concentration of 0.15 mM seemed to be inhibited. Moreover, the H_2O_2 in this case plays the role of an inhibiting agent at an excess of concentration and it can react with the hydroxyl radicals generated during the photo-Fenton reaction to compete with the oxidant, it may promote secondary reactions that consume H_2O_2 and therefore inhibit the SG degradation according to the following reaction [42]:

$$H_2O_2 + -OH_2\ O_2 + -OH \leftrightarrow HO_{2-} + H_2O\ k = 3 \times 10^7 7\ mol^{-1}.L.S^{-1} \quad (13)$$

Hence 0.15 mM of H_2O_2 was noticed as an appropriate concentration with the optimal conditions: 0.15 mM of Fe(III) and a molar ratio of 2, with an initial SG dye pollutant concentration of 10 mg/L. H_2O_2 can be produced in solution, with the following pattern. We can see in Fig. 11 that the consumption of H_2O_2 can be successful because of its in situ production.

3.9. Effects of ions for the two processes involved (Fe(III)/Lig) and (Fe (II)/Lig)

The composition of renal effluents is very complex and may contain a wide range of organic and inorganic ions in varying concentrations. The presence of these ions may affect the concentration of hydroxyl radicals during a photo-Fenton reaction and may retard or inhibit the degradation activity of the pollutant [44].

In this part of the work, we have evaluated the effect of some inorganic and inorganic ions that existed in salts form on the photo-Fenton oxidation of SG dye, the salts used are sodium chlorides NaCl, sodium sulfates Na_2SO_4, sodium bicarbonates $NaHCO_3$ and potassium nitrates KNO_3 at different concentrations 10, 50 and 100 mM. However, the other operating conditions are kept fixed at 0.15 mM of Fe(III), 2 of molar ratio and 10 mg/L of SG dye pollutant concertation for both cases, the complex (Fe(III)/Lig) as well as, a Fe(II)/Lig concentration of 0.2 mM, a molar ratio of 2, an H_2O_2 concentration of 0.15 mM and a pollutant concertation of 10 mg/L. The effect of ions on the rate of photo-Fenton efficiency is summarized in Fig. 12.

The effect rate efficiency of sulfate, chloride, bicarbonate and nitrate ions with different concentrations on the photo-Fenton degradation of SG dye is presented in Fig. 12. As can be observed an overall effect of a decrease in the photo-Fenton activity for the degradation of GS dye in all added ions, this behavior can be explained by the reaction of ions with the formed hydroxyl radicals. In addition, chloride, sulfate and nitrate form a complex with Fe(II) and Fe(III) enabling to produce of hydroxyl radicals.

According to Fig. 12, concerning the complex (Fe(III)/Lig), a non-significant effect was observed for the sulfates. However, for the other ions a rather important inhibition was reported especially for the bicarbonates, it was noticed a decrease in the photodegradation yield of

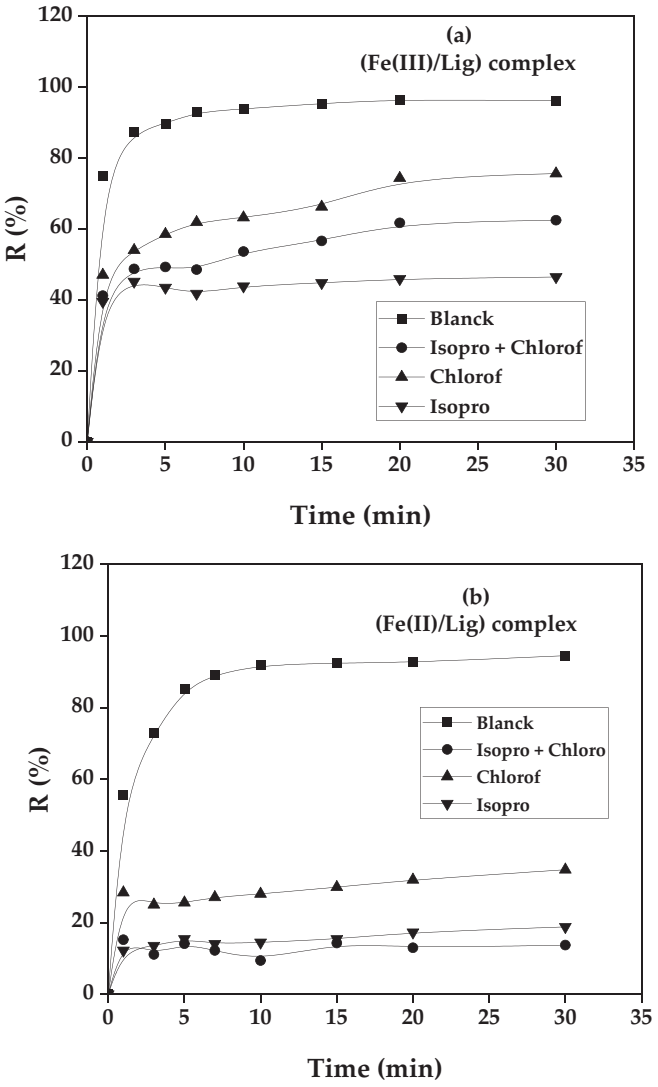

Fig. 13. Photo-fenton degradation of SG in the presence of scavengers for both complexes, a: Case of the (Fe(III)/Lig) complex, b: Case of the (Fe(II)/Lig) complex for time = 30 min [VS]o = 10 mg/L, [Fe(II)]o = [Fe(III)]o = 0.2 mM, R = 2, [H_2O_2]o = 0.15 mM, [isop]o = [chlor]o = 1 M.

Table 7
The analyses of the kinetic models applied for the two complexes (Fe(III)/Lig) (Fe(II)/Lig).

	Complex Fe(III)/Lig		Complex Fe(II)/Lig	
	1st order	2nd order	1st order	2nd order
R^2	0.6854	0.9684	0.5306	0.972
Rate kinetic k	$k_1 = 0.4894$ (1/min)	$k_2 = 0.1447$ (L./mg min)	$k_1 = 0.1686$ (1/min)	$k_2 = 0.126$ (L./mg min)

86.29% for the concentration of 100 mM. On the other hand, for the chloride and the nitrate, a decrease of 22.32% and 15.12% respectively was noted for the same dye SG initial concentration (100 mM).

Concerning the system of complex (Fe(II)/Lig), a slight inhibition of 1.79% was marked for chlorides at a concentration of 100 mM. However, the same observations were noted for the first complex with the bicarbonate had a drastic inhibition with a decrease of 91% in photodegradation yield for 100 mM concentration.

Moreover, the addition of chloride ions up to 100 mM tends to

influence the photodegradation activity. In similar cases, when chloride ions are added to the solution, they act as a scavenger by trapping the hydroxyl radicals [45]. This trend can be explained by the reaction with radical hydroxyl as mentioned by the following reaction [46]:

$$HO^{\cdot} + Cl^{-} \rightarrow ClOH \; k = 4.3 \times 10^{9}\ M^{-1}\ s^{-1} \quad (14)$$

The photo-Fenton degradation of the SG dye was considerably decreased in the presence of bicarbonate ion HCO_3^-, this can be explained by the hydroxyl scavenging properties of carbonates ions. In addition, bicarbonate of sodium is a more stable ion that can play a role in changing pH medium. Hence, another produced radical $CO_3^{\bullet -}$ in the scavenging reaction (15) in the hydroxyl radical ($OH^{\bullet}$) has lower photocatalytic reactivity than hydroxyl radical [47].

$$HO^{\cdot} + HCO^{3-} \rightarrow CO^{3-\cdot} + H_2O \; k = 8.5 \times 10^{6}\ M^{-1}\ s^{-1} \quad (15)$$

3.10. Effect of scavengers

The previous studies of photo-Fenton reaction investigated the effect of different scavengers as an important reagent in the reaction system to confirm the intervention of different active radicals.

To study the influence of the presence of scavengers in the photo-Fenton oxidation of SG dye in the case of complex (Fe(III)/Lig and (Fe (II)/Lig complexes, we used isopropanol (Isop), chloroform (chlor) and their mixture. According to previous studies, isopropanol reacts with hydroxyl radicals with a reaction rate of 1.9×10^9 M-1 s^{-1} [48]. For the superoxide radicals, the scavenger used is chloroform which reacts with O_2^- with a reaction rate of $9.6 \times 10^8\ M^{-1}\ s^{-1}$, thereby it can also react with $HO^{\bullet}$ with a reaction rate of $7 \times 10^6\ M^{-1}\ s^{-1}$ [49]. The obtained results are illustrated in Fig. 13a and b:

The effect of isopropanol, chloride and the mixture isopro+ chlor on the photo-Fenton reaction of SG dye is investigated in Fig. 13 for both the complex (Fe(III)/Lig) and the complex (Fe(II)/Lig) cases.

It is noted that with the addition of the two scavengers at the beginning of the reaction for a concentration of 1 mol a significant inhibition was noticed. This can be explained by the fact that the elimination of our SG dye is due on one hand to the production of hydroxyl radicals with a percentage of 40.2% and on the other hand to superoxide radicals with a percentage of 24.7%, for the first system of complex (Fe (III)/Lig) and a percentage of 80. 7% is reached with a production of 14.7% of hydroxyl radicals and superoxide radicals with the second system of complex (Fe(II)/Lig). However, the remaining photo-Fenton degradation percentage can be due to the oxalate radicals produced in situ during the reaction in both processes [50].

3.11. Kinetic study of the degradation of GS dye with complex (Fe(III)/Lig) and (Fe(II)/Lig) system

In this part, to determine the degradation kinetics of SG dye by modified photo-Fenton oxidation for the system with complexes (Fe (III)/Lig) and (Fe(II)/Lig), respectively. Moreover, the first-order and second-order kinetics models given by the eqs. (11 and 12) are applied and analyzed using the coefficient of determination (R^2) value [51]. Thereafter, the model with the best fit of experiment data was selected.

For the complex (Fe(III)/Lig): SG dye concentration: 10 mg/L, Fe(III) concentration: 0.15 mM, Molar ratio: 2, For the complex (Fe(II)/Lig): SG dye concentration: 10 mg/L, Fe(II) concentration: 0.2 mM, Molar ratio: 2 and H_2O_2: 0.15 mM.

$$C_t = C_o - e^{k1t} \quad (16)$$

$$1 \Big/ C_t = \frac{1}{C_o} - k_2 t \quad (17)$$

Where;

Ct is the concentration at time t, Co is the initial SG dye concentration, t is the reaction time, and k1, and k2 are the first and second-order reaction kinetic rate constants, respectively. The various obtained kinetic parameters and regression coefficients (R^2) for each reaction model were analyzed, and the results are presented in Table 7.

The photo-Fenton reaction rate constants are calculated from the slope of the kinetic model plots. Examining the data 7 and according to the comparison of the R^2 values of the plots, it was revealed that the modified photo-Fenton reaction of the SG dye follows the second-order kinetic model for Fe(III)/Lig and Fe(II)/Lig complexes with an R^2 of 96.84% and 97.2% respectively. We can conclude that the decolorization kinetics is well presented by the second-order model in the two studied processes. Further, the kinetics constant of second-order reaction k_2 was notably influenced by the nature of the complex. This investigation may associated with the generation of OH* radical which is highly produced with ferrioxalate complex (Fe(III)/Lig) [52]; Finally, several additional studies found in the literature corroborate our finding that the photo-Fenton reaction proceeds according to second-order kinetics.

4. Conclusion

This research study focused on the removal efficiency of SG food dye degradation by a modified homogenous photo-Fenton process under a sustainable natural light source. The influence of various operating conditions such as light source, Fe(II)/(III) concentrations, oxalic acid concentration as ligand, pH medium and hydrogen peroxide concentration were investigated in detail. It was observed that the first important results obtained from preliminary tests confirmed the absence of undesirable reactions, while sunlight proved its efficiency for improving the degradation rate of SG dye which decreased the cost of energy consumption.

It should be mentioned that the classical photo-Fenton reaction is favorable at an acidic medium (pH = 3). However, the addition of oxalic acid demonstrated that this reaction could be performed in a wide range of pH close to the neutrality and it depends only on the initial SG dye concentration, iron catalyst amount, ligand concentration and hydrogen peroxide concentration. In addition, the obtained results proved that both complexes of Fe(II)/lig and Fe(III)/Lig demonstrated their efficiency for the SG degradation removal with a slight enhancement for Fe (III)/Lig complex. Under sunlight, the ferrioxalate complex can be photo-activated and lead to a reduction of the Fe(III) to Fe(II) initiating the generation of radicals through the reaction with hydrogen peroxide. The Box-Benhken experimental design (BBD) was applied for developing a mathematical model and optimizing the photo-Fenton process to get more insight information. BBD is combined with response surface methodology to reveal the effect of independent variables and their interactions on the response variables. The effect of ions such as chloride, nitrate and bicarbonate was also determined in the performed experiments. It was found that some ions exhibited an important inhibition role in the degradation reaction and reduced the generating rate of hydroxyl radicals from photo-Fenton reagents. For the bicarbonates, it was noticed the SG degradation yield decreased by 9.76% and 3.96% for Fe(III)/lig and Fe(II)/lig complexes, respectively. On the other hand, for the chloride 73.73% and 93.17% reduction in the SG degradation yield was observed for Fe(III)/lig and Fe(II)/lig complexes, respectively, and the reductions under nitrate are 80.93% and 94.7% for Fe(III)/lig and Fe(II)/lig, respectively. The same behavior is obtained by adding isopropanol which plays the role of electron acceptors such as H_2O_2. These findings are highly encouraging for the use of the modified photo-Fenton process for the removal of organic pollutants from effluent to protect the aquatic environment.

CRediT authorship contribution statement

Mohammed Kebir: Conceptualization, Methodology, Software, Validation, Formal analysis, Investigation, Resources, Data curation,

Writing – original draft, Visualization, Project administration. **Imen-Kahina Benramdhan**: Conceptualization, Methodology, Software, Investigation, Resources, Data curation. **Noureddine Nasrallah**: Conceptualization, Methodology, Investigation, Resources, Writing – review & editing, Visualization, Supervision, Project administration. **Hichem Tahraoui**: Conceptualization, Software, Validation, Formal analysis, Investigation, Data curation, Writing – original draft, Visualization. **Nadia Bait**: Conceptualization, Methodology, Investigation, Resources, Writing – review & editing, Visualization. **Houssine Benaissa**: Conceptualization, Validation, Formal analysis, Investigation, Resources, Writing – review & editing, Visualization. **Rachid Ameraoui**: Conceptualization, Methodology, Formal analysis, Investigation, Resources, Writing – review & editing, Visualization. **Jie Zhang**: Conceptualization, Software, Validation, Investigation, Data curation, Writing – review & editing, Visualization, Project administration. **Aymen Amin Assadi**: Conceptualization, Validation, Investigation, Writing – review & editing, Visualization. **Lotfi Mouni**: Conceptualization, Validation, Writing – review & editing, Visualization. **Abdeltif Amrane**: Conceptualization, Methodology, Software, Validation, Formal analysis, Investigation, Resources, Data curation, Writing – original draft, Writing – review & editing, Visualization, Supervision, Project administration.

Declaration of Competing Interest

The authors declare that they have no known competing financial interests or personal relationships that could have appeared to influence the work reported in this paper.

Data availability

Data will be made available on request.

References

[1] M. Compton, S. Willis, B. Rezaie, K. Humes, Food processing industry energy and water consumption in the Pacific northwest, Innovative Food Sci. Emerg. Technol. 47 (2018) 371–383, https://doi.org/10.1016/j.ifset.2018.04.001.

[2] K. Obaideen, N. Shehata, E.T. Sayed, M.A. Abdelkareem, M.S. Mahmoud, A. G. Olabi, The role of wastewater treatment in achieving sustainable development goals (SDGs) and sustainability guideline, Energy Nexus. 7 (2022), 100112, https://doi.org/10.1016/j.nexus.2022.100112.

[3] V.H.T. Pham, J. Kim, S. Chang, D. Bang, Investigating bio-inspired degradation of toxic dyes using potential multi-enzyme producing extremophiles, Microorganisms. 11 (2023) 1273, https://doi.org/10.3390/microorganisms11051273.

[4] L. Zhang, X. Bi, Z. Wang, A.S. Ertürk, G. Elmaci, H. Zhao, P. Zhao, X. Meng, Brønsted-acid sites promoted degradation of phthalate esters over MnO2: mineralization enhancement and aquatic toxicity assessment, Chemosphere. 291 (2022), 132740.

[5] B. Koul, N. Bhat, M. Abubakar, M. Mishra, A.P. Arukha, D. Yadav, Application of natural coagulants in water treatment: a sustainable alternative to chemicals, Water. 14 (2022) 3751, https://doi.org/10.3390/w14223751.

[6] L. Clarizia, D. Russo, I. Di Somma, R. Marotta, R. Andreozzi, Homogeneous photo-Fenton processes at near neutral pH: a review, Appl. Catal. B Environ. 209 (2017) 358–371, https://doi.org/10.1016/j.apcatb.2017.03.011.

[7] A.S. Ertürk, G. Elmaci, M.U. Gürbüz, Reductant free green synthesis of magnetically recyclable MnFe2O4@ SiO2-Ag core-shell nanocatalyst for the direct reduction of organic dye pollutants, Turk. J. Chem. 45 (2021) 1968–1979.

[8] R.R. Navarro, H. Ichikawa, K. Tatsumi, Ferrite formation from photo-Fenton treated wastewater, Chemosphere. 80 (2010) 404–409.

[9] I.K. Benramdane, N. Nasrallah, A. Amrane, M. Kebir, M. Trari, F. Fourcade, A. A. Assadi, R. Maachi, Optimization of the artificial neuronal network for the degradation and mineralization of amoxicillin photoinduced by the complex ferrioxalate with a gradual and progressive approach of the ligand, J. Photochem. Photobiol. A Chem. 406 (2021), 112982, https://doi.org/10.1016/j.jphotochem.2020.112982.

[10] Y.-J. Zhang, J.-J. Chen, G.-X. Huang, W.-W. Li, H.-Q. Yu, M. Elimelech, Distinguishing homogeneous advanced oxidation processes in bulk water from heterogeneous surface reactions in organic oxidation, Proc. Natl. Acad. Sci. U. S. A. 120 (2023), e2302407120, https://doi.org/10.1073/pnas.2302407120.

[11] L. Xu, L. Qi, Y. Han, W. Lu, J. Han, W. Qiao, X. Mei, Y. Pan, K. Song, C. Ling, L. Gan, Improvement of Fe2+/peroxymonosulfate oxidation of organic pollutants by promoting Fe2+ regeneration with visible light driven g-C3N4 photocatalysis, Chem. Eng. J. 430 (2022), 132828, https://doi.org/10.1016/j.cej.2021.132828.

[12] Y. Liu, H. Zhou, K. Wei, C. He, Y. Du, Y. Liu, R. Xie, G. Yao, B. Lai, Extending semiconductor-based photo-Fenton reaction to circumneutral pH using chelating agents: the overlooked role of pH on the reduction mechanism of Fe3+, Chem. Eng. J. 450 (2022), 138109.

[13] L.I. Doumic, P.A. Soares, M.A. Ayude, M. Cassanello, R.A. Boaventura, V.J. Vilar, Enhancement of a solar photo-Fenton reaction by using ferrioxalate complexes for the treatment of a synthetic cotton-textile dyeing wastewater, Chem. Eng. J. 277 (2015) 86–96.

[14] Z. Ye, I. Sirés, H. Zhang, Y.-H. Huang, Mineralization of pentachlorophenol by ferrioxalate-assisted solar photo-Fenton process at mild pH, Chemosphere. 217 (2019) 475–482.

[15] A. Garg, G. Kaur, V.K. Sangal, P.K. Bajpai, S. Upadhyay, Optimization methodology based on neural networks and box-behnken design applied to photocatalysis of acid red 114 dye, Environ. Eng. Res. 25 (2019) 753–762, https://doi.org/10.4491/eer.2019.246.

[16] M. Dissanayake, N. Liyanage, C. Herath, S. Rathnayake, E.Y. Fernando, Mineralization of persistent azo dye pollutants by a microaerophilic tropical lake sediment mixed bacterial consortium, Environ. Adv. 3 (2021), 100038, https://doi.org/10.1016/j.envadv.2021.100038.

[17] N. Bouchelkia, H. Tahraoui, A. Amrane, H. Belkacemi, J.-C. Bollinger, A. Bouzaza, A. Zoukel, J. Zhang, L. Mouni, Jujube stones based highly efficient activated carbon for methylene blue adsorption: kinetics and isotherms modeling, thermodynamics and mechanism study, optimization via response surface methodology and machine learning approaches, Process. Saf. Environ. Prot. (2022).

[18] H. Tahraoui, A.-E. Belhadj, A. Hamitouche, M. Bouhedda, A. Amrane, Predicting the concentration of sulfate (SO42-) in drinking water using artificial neural networks: a case study: Médéa-Algeria, Desalin. Water Treat. 217 (2021) 181–194, https://doi.org/10.5004/dwt.2021.26813.

[19] H. Tahraoui, A. Amrane, A.-E. Belhadj, J. Zhang, Modeling the organic matter of water using the decision tree coupled with bootstrap aggregated and least-squares boosting, Environ. Technol. Innov. 27 (2022), 102419, https://doi.org/10.1016/j.eti.2022.102419.

[20] H. Tahraoui, A.E. Belhadj, A.E. Hamitouche, Prediction of the bicarbonate amount in drinking water in the region of Médéa using artificial neural network modelling, Kem. Indust. 69 (2020) 595–602, https://doi.org/10.15255/KUI.2020.002.

[21] A. Bousselma, D. Abdessemed, H. Tahraoui, A. Amrane, Artificial intelligence and mathematical modelling of the drying kinetics of pre-treated whole apricots, Kem. Indust. (2021), https://doi.org/10.15255/KUI.2020.079.

[22] M.M. Yahoum, S. Toumi, S. Hentabli, H. Tahraoui, S. Lefnaoui, A. Hadjsadok, A. Amrane, M. Kebir, N. Moula, A.A. Assadi, Experimental analysis and neural network modeling of the rheological behavior of xanthan gum and its derivatives, Materials. 16 (2023) 2565.

[23] M. Zamouche, M. Chermat, Z. Kermiche, H. Tahraoui, M. Kebir, J.-C. Bollinger, A. Amrane, L. Mouni, Predictive model based on K-nearest neighbor coupled with the gray wolf optimizer algorithm (KNN_GWO) for estimating the amount of phenol adsorption on powdered activated carbon, Water. 15 (2023) 493.

[24] M. Zamouche, H. Tahraoui, Z. Laggoun, S. Mechati, R. Chemchmi, M.I. Kanjal, A. Amrane, A. Hadadi, L. Mouni, Optimization and prediction of stability of emulsified liquid membrane (ELM): artificial neural network, Processes. 11 (2023) 364.

[25] H. Tahraoui, A.-E. Belhadj, A. Amrane, E.H. Houssein, Predicting the concentration of sulfate using machine learning methods, Earth Sci. Inf. 15 (2022) 1023–1044, https://doi.org/10.1007/s12145-022-00785-9.

[26] A. Hadadi, A. Imessaoudene, J.-C. Bollinger, A. Bouzaza, A. Amrane, H. Tahraoui, L. Mouni, Aleppo pine seeds (Pinus halepensis Mill.) as a promising novel green coagulant for the removal of Congo red dye: optimization via machine learning algorithm, J. Environ. Manag. 331 (2023), 117286.

[27] H. Tahraoui, S. Toumi, A.H. Hassein-Bey, A. Bousselma, A.N.E.H. Sid, A.-E. Belhadj, Z. Triki, M. Kebir, A. Amrane, J. Zhang, Advancing water quality research: K-nearest neighbor coupled with the improved Grey wolf optimizer algorithm model unveils new possibilities for dry residue prediction, Water. 15 (2023) 2631.

[28] H. Tahraoui, A.-E. Belhadj, Z. Triki, N.R. Boudella, S. Seder, A. Amrane, J. Zhang, N. Moula, A. Tifoura, R. Ferhat, A. Bousselma, N. Mihoubi, Mixed Coagulant-Flocculant Optimization for Pharmaceutical Effluent Pretreatment Using Response Surface Methodology and Gaussian Process Regression, Process Safety and Environmental Protection, 2022, https://doi.org/10.1016/j.psep.2022.11.045.

[29] M. Nedjhioui, N. Nasrallah, M. Kebir, H. Tahraoui, R. Bouallouche, A.A. Assadi, A. Amrane, B. Jaouadi, J. Zhang, L. Mouni, Designing an efficient surfactant–polymer–oil–electrolyte system: a multi-objective optimization study, Processes. 11 (2023) 1314.

[30] H. Tahraoui, A.E. Belhadj, N. Moula, S. Bouranene, A. Amrane, Optimisation and prediction of the coagulant dose for the elimination of organic micropollutants based on turbidity, Kem. Ind. (2021), https://doi.org/10.15255/KUI.2021.001.

[31] A. Imessaoudene, S. Cheikh, A. Hadadi, N. Hamri, J.-C. Bollinger, A. Amrane, H. Tahraoui, A. Manseri, L. Mouni, Adsorption performance of zeolite for the removal of Congo red dye: factorial design experiments, Kinetic Equilib. Stud. Separ. 10 (2023) 57, https://doi.org/10.3390/separations10010057.

[32] A.J. Luna, O. Chiavone-Filho, A. Machulek, J.E.F. De Moraes, C.A.O. Nascimento, Photo-Fenton oxidation of phenol and organochlorides (2,4-DCP and 2,4-D) in aqueous alkaline medium with high chloride concentration, J. Environ. Manag. 111 (2012) 10–17, https://doi.org/10.1016/j.jenvman.2012.06.014.

[33] S. Hussain, E. Aneggi, D. Goi, Catalytic activity of metals in heterogeneous Fenton-like oxidation of wastewater contaminants: a review, Environ. Chem. Lett. 19 (2021) 2405–2424, https://doi.org/10.1007/s10311-021-01185-z.

[34] I. Ghoul, N. Debbache, B.A. Dekkiche, N. Seraghni, T. Sehili, Z. Marin, J. A. Santaballa, M. Canle, Fe (III)-citrate enhanced sunlight-driven photocatalysis of aqueous carbamazepine, J. Photochem. Photobiol. A Chem. 378 (2019) 147–155.
[35] R. Girón-Navarro, V. Martínez-Miranda, E.A. Teutli-Sequeira, I. Linares-Hernández, I.G. Martínez-Cienfuegos, M. Sánchez-Pozos, F. Santoyo-Tepole, A solar photoFenton process with calcium peroxide from eggshell and ferrioxalate complexes for the degradation of the commercial herbicide 2,4-D in water, J. Photochem. Photobiol. A Chem. 438 (2023), 114550, https://doi.org/10.1016/j.jphotochem.2023.114550.
[36] A.H. Panahi, S.D. Ashrafi, H. Kamani, M. Khodadadi, E.C. Lima, F.K. Mostafapour, A.H. Mahvi, Removal of cephalexin from artificial wastewater by mesoporous silica materials using box-Behnken response surface methodology, Desalin, Desalin. Water Treat. 159 (2019) 169–180.
[37] A. Nath, P.K. Chattopadhyay, Optimization of oven toasting for improving crispness and other quality attributes of ready to eat potato-soy snack using response surface methodology, J. Food Eng. 80 (2007) 1282–1292.
[38] Z.N. Garba, A.A. Rahim, Process optimization of K2C2O4-activated carbon from Prosopis africana seed hulls using response surface methodology, J. Anal. Appl. Pyrolysis 107 (2014) 306–312.
[39] S. Lefnaoui, N. Moulai-Mostefa, Investigation and optimization of formulation factors of a hydrogel network based on kappa carrageenan–pregelatinized starch blend using an experimental design, Colloids Surf. A Physicochem. Eng. Asp. 458 (2014) 117–125.
[40] A. Zaher, Photo-catalytic degradation of phenol wastewater: optimization using response surface methodology, Egypt. J. Chem. 63 (2020) 4439–4445.
[41] A. Srivastav, T. Rawat, J. Singh, S. Nawaz, Multiobjective Grey Wolf optimization based allocation of SVC in power system, in: 2022 2nd International Conference on Innovative Sustainable Computational Technologies (CISCT), IEEE, 2022, pp. 1–5.
[42] G.V. Buxton, C.L. Greenstock, W.P. Helman, A.B. Ross, Critical review of rate constants for reactions of hydrated electrons, hydrogen atoms and hydroxyl radicals (·OH/·O $^-$) in aqueous solution, J. Phys. Chem. Ref. Data Monogr. 17 (1988) 513–886, https://doi.org/10.1063/1.555805.
[43] J.L. Wang, L.J. Xu, Advanced oxidation processes for wastewater treatment: formation of hydroxyl radical and application, Crit. Rev. Environ. Sci. Technol. 42 (2012) 251–325, https://doi.org/10.1080/10643389.2010.507698.
[44] A. Machulek, J.E.F. Moraes, L.T. Okano, C.A. Silvérioc, F.H. Quina, Photolysis of ferric ions in the presence of sulfate or chloride ions: implications for the photo-Fenton process, Photochem. Photobiol. Sci. 8 (2009) 985–991, https://doi.org/10.1039/b900553f.
[45] C.-H. Liao, S.-F. Kang, F.-A. Wu, Hydroxyl radical scavenging role of chloride and bicarbonate ions in the H2O2/UV process, Chemosphere. 44 (2001) 1193–1200, https://doi.org/10.1016/S0045-6535(00)00278-2.
[46] L.G. Devi, C. Munikrishnappa, B. Nagaraj, K.E. Rajashekhar, Effect of chloride and sulfate ions on the advanced photo Fenton and modified photo Fenton degradation process of alizarin red S, J. Mol. Catal. A Chem. 374–375 (2013) 125–131, https://doi.org/10.1016/j.molcata.2013.03.023.
[47] J. Khan, M. Tariq, M. Muhammad, M.H. Mehmood, I. Ullah, A. Raziq, F. Akbar, M. Saqib, A. Rahim, A. Niaz, Kinetic and thermodynamic study of oxidative degradation of acid yellow 17 dye by Fenton-like process: effect of HCO3−, CO32−, Cl− and SO42− on dye degradation, Bull. Chem. Soc. Ethiop. 33 (2019) 243, https://doi.org/10.4314/bcse.v33i2.5.
[48] G. Cheng, J. Wan, Q. Li, L. Sun, Y. Zhang, Z. Li, C. Dang, J. Fu, Degradation of reactive brilliant red X-3B by photo-Fenton-like process: effects of water chemistry factors and degradation mechanism, Water. 14 (2022) 380, https://doi.org/10.3390/w14030380.
[49] D.S. Vavilapalli, S. Behara, R.G. Peri, T. Thomas, B. Muthuraaman, M.S.R. Rao, S. Singh, Enhanced photo-Fenton and photoelectrochemical activities in nitrogen doped brownmillerite KBiFe2O5, Sci. Rep. 12 (2022) 5111, https://doi.org/10.1038/s41598-022-08966-8.
[50] L. Hu, P. Wang, S. Xiong, S. Chen, X. Yin, L. Wang, H. Wang, The attractive efficiency contributed by the in-situ reactivation of ferrous oxalate in heterogeneous Fenton process, Appl. Surf. Sci. 467–468 (2019) 185–192, https://doi.org/10.1016/j.apsusc.2018.10.151.
[51] D.R. Ramírez-Carranza, G. Macedo-Miranda, G. González-Blanco, S. Mireya-Martínez, J.C. González-Juárez, R. Beristain-Cardoso, Effect of Fe (II) concentration on metronidazole degradation by Fenton process: performance and kinetic study, MRS Adv. 5 (2020) 3265–3272, https://doi.org/10.1557/adv.2020.406.
[52] M.M. Nour, M.A. Tony, H.A. Nabwey, Heterogeneous Fenton oxidation with natural clay for textile Levafix dark blue dye removal from aqueous effluent, Appl. Sci. 13 (2023) 8948.